

U-Pb geochronology of volcanic rocks from the Jurassic Talkeetna Formation and detrital zircons from prearc and postarc sequences: Implications for the age of magmatism and inheritance in the Talkeetna arc

Jeffrey M. Amato*

Department of Geological Sciences, New Mexico State University, Las Cruces, New Mexico 88003, USA

Matthew E. Rioux*

Department of Geological Sciences, University of California, Santa Barbara, California 93106, USA

Peter B. Kelemen

Department of Earth and Environmental Sciences, Lamont-Doherty Earth Observatory, Palisades, New York 10964, USA

George E. Gehrels

Department of Geosciences, University of Arizona, Tucson, Arizona 85721, USA

Peter D. Clift

School of Geosciences, University of Aberdeen, Aberdeen, UK

Terry L. Pavlis

Department of Geological Sciences, University of Texas, El Paso, Texas 79968, USA

Amy E. Draut

Department of Earth Sciences, University of California, Santa Cruz, California 95064, USA

ABSTRACT

Six samples collected from pre-, syn-, and post-Talkeetna arc units in south-central Alaska were dated using single-grain zircon LA-MC-ICP-MS geochronology to assess the age of arc volcanism and the presence and age of any inherited components in the arc. The oldest dated sample comes from a volcanic breccia at the base of the Talkeetna Formation on the Alaska Peninsula and indicates that initial arc volcanism began by 207 ± 5 Ma. A sedimentary rock overlying the volcanic section in the Talkeetna Mountains has a maximum depositional age of <167 Ma. This is in agreement with biochronologic ages for the top of the Talkeetna Formation, suggesting that the Talkeetna arc was active for ca. 40 m.y.

*E-mail, Amato: amato@nmsu.edu. Present address, Rioux: Department of Earth, Atmospheric and Planetary Sciences, Massachusetts Institute of Technology, Cambridge, Massachusetts, 02139, USA.

Amato, J.M., Rioux, M.E., Kelemen, P.B., Gehrels, G.E., Clift, P.D., Pavlis, T.L., and Draut, A.E., 2007, U-Pb geochronology of volcanic rocks from the Jurassic Talkeetna Formation and detrital zircons from prearc and postarc sequences: Implications for the age of magmatism and inheritance in the Talkeetna arc, *in* Ridgway, K.D., Trop, J.M., Glen, J.M.G., and O'Neill, J.M., eds., *Tectonic Growth of a Collisional Continental Margin: Crustal Evolution of Southern Alaska*: Geological Society of America Special Paper 431, p. 253–271, doi: 10.1130/2007.2431(11). For permission to copy, contact editing@geosociety.org. ©2007 The Geological Society of America. All rights reserved.

Three samples from interplutonic screens and roof pendants in the Jurassic batholith on the Alaska Peninsula provide information about the tectonic setting of Talkeetna arc magmatism. All three samples contain Paleozoic to Proterozoic zircons and require that arc magmas on the Alaska Peninsula intruded into detritus that contained older continental zircons. This finding is distinct from observations from eastern exposures of the arc in the Chugach and Talkeetna Mountains, where there is only limited evidence for pre-Paleozoic zircons, and it suggests that there were along-strike variations in the tectonic setting of the arc.

Keywords: detrital zircons, Talkeetna Formation, Alaska, magmatism, sedimentation.

INTRODUCTION

The Peninsular Terrane of southern Alaska consists of the Jurassic Talkeetna arc, prearc oceanic rocks, and overlying sedimentary sequences (Jones et al., 1987; Plafker et al., 1989). It accreted to western North America during Mesozoic time (Trop et al., 2002; Clift et al., 2005b). The exposed arc rocks include ultramafic to mafic cumulates, mafic plutonic rocks, intermediate to felsic plutonic rocks, and the Jurassic Talkeetna Formation. These units are interpreted to represent a rare cross section from the subarc mantle to subaerial volcanic rocks of an intraoceanic arc, and as a result the Talkeetna arc is considered a type section of intraoceanic arc crust (Burns, 1985; DeBaro and Coleman, 1989; Rioux et al., 2007).

We used laser-ablation multicollector inductively coupled plasma mass spectrometry (LA-MC-ICP-MS) to date zircons from pre-, syn-, and postarc rocks in southern Alaska (Fig. 1). The goals of this study were to address these questions: (1) do the pre- and synarc rocks of the Peninsular Terrane contain evidence for older terrestrially derived clastic material that could be a possible contaminant for arc magmas passing through these rocks, and (2) can the ages of zircons in pre-, syn-, and postarc sedimentary rocks be used to constrain the timing of Talkeetna arc volcanism?

The advent of LA-MC-ICP-MS has facilitated the analysis of U-Pb ages from detrital zircons, allowing for rapid determination of 100 ages from a sample in less than five hours. Application of this geochronologic tool can be used to quickly assess the presence of contamination, the ages of source rocks, and the maximum depositional ages of sedimentary rocks.

We focused on six metasedimentary, igneous, and sedimentary samples from the Katmai, Iliamna, Kenai, Anchorage, and Talkeetna Mountains 1:250,000 quadrangles of southern Alaska. Five of these are quartz-rich sedimentary or low-grade metamorphic rocks from volcanic sources. The sixth sample is from a green-schist-facies metabasalt in the western Chugach Mountains. This study complements an ongoing comprehensive investigation of the age, geochemistry, and evolution of the Talkeetna island arc (e.g., Clift et al., 2005a; 2005b; Rioux et al., 2007; Greene et al., 2006).

REGIONAL SETTING

The rocks in this study were collected from various units within the Peninsular Terrane (Fig. 1), an allochthonous lithostrati-

graphic unit that accreted to North America in the latest Jurassic or early Cretaceous (Trop et al., 2005; Clift et al., 2005b). The Peninsular Terrane is tectonically juxtaposed with the Chugach and Wrangellia Terranes and is separated from the Chugach Terrane by the Border Ranges Fault system (e.g., Pavlis, 1982, 1983), which is interpreted to be a paleosubduction-thrust that was reactivated

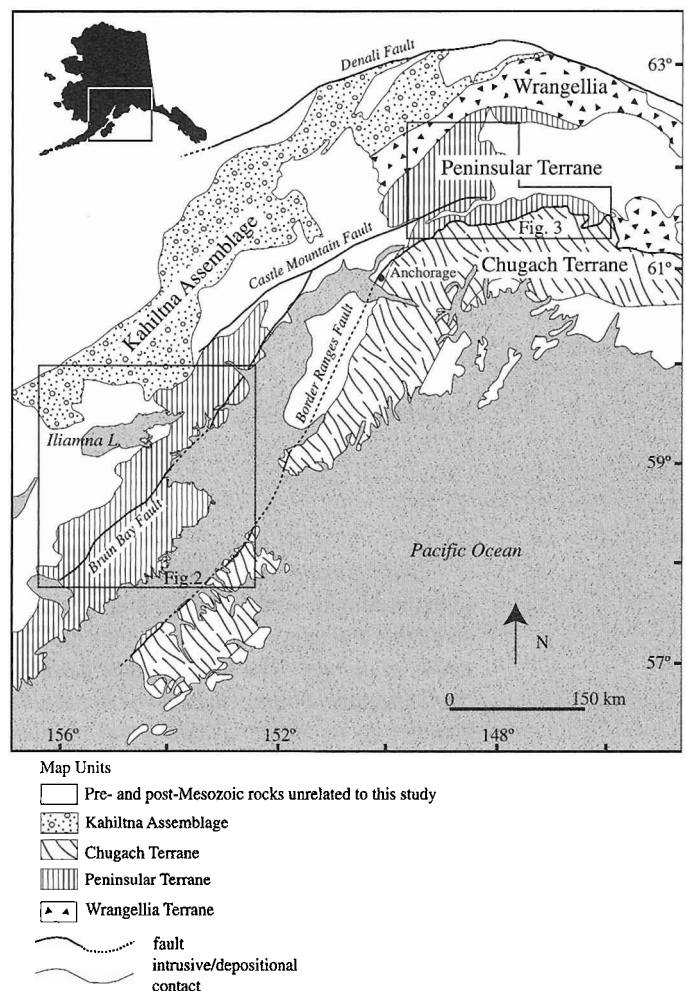


Figure 1. Tectonic map of southern Alaska showing the Wrangellia, Peninsular, Kahiltina, and Chugach Terranes and the locations of Figures 2 and 3. Modified after Silberling et al. (1994).

as a right-lateral strike-slip fault during the Cenozoic (Clift et al., 2005b). The Peninsular Terrane includes Triassic prearc oceanic basement, the Jurassic Talkeetna island arc, and overlying sedimentary successions. No Precambrian crust is known to be part of this terrane, and the Talkeetna arc is a typical example of an intra-oceanic arc. Subduction during arc magmatism is considered to have been north-dipping (present coordinates) based on the presence of back-arc volcanic rocks to the north of the main part of the arc and Early Jurassic blueschists to the south of the arc (Sisson and Onstott, 1986; Roeske et al., 1989; Clift et al., 2005a, 2005b). The exposed arc section now dips northward, exposing ultramafic arc basement to the south and the upper crustal volcanic rocks to the north. Significant right-lateral strike-slip faulting has obscured many original relationships between these terranes.

The rocks of the Peninsular terrane can be broadly grouped into pre-, syn-, and post-Talkeetna arc units. Precambrian successions in southwest Alaska include the Kakhonak Complex, Cottonwood Bay Greenstone, and Kamishak Formation mainly exposed in the Iliamna quadrangle (Detterman and Reed, 1980), the Tlikakila Complex in the Lake Clark region (Wallace et al., 1989; Amato et al., this volume, chapter 10), and metamorphic rocks of the Knik River Terrane that were intruded by Jurassic plutons in the western Chugach Mountains (Pavlis et al., 1988). Synarc rocks are represented by the volcanic and volcanoclastic Talkeetna Formation (Newberry et al., 1986; Clift et al., 2005a) and Jurassic arc plutonic rocks, including intermediate to felsic-composition intrusions, gabbro (norites), and ultramafic arc lower crust (Reed and Lanphere, 1973; Burns, 1985; DeBari and Coleman, 1989). Postarc sedimentary rocks include the Tuxedni Group and other Middle Jurassic sedimentary rocks such as the Chinitina (or Chinitna) Formation (Detterman and Reed, 1980; Trop et al., 2005).

Precambrian Succession

The Kakhonak Complex (Detterman and Reed, 1980) includes a diverse suite of Triassic–Jurassic (and possibly Permian) greenschist facies sedimentary and igneous rocks. Typical rock types are metamorphosed argillite, marble, quartzite, and quartz-mica schist (Detterman and Reed, 1980). These rocks are generally found as roof pendants in the Jurassic and younger granitic plutons in the eastern Iliamna and western Kenai quadrangles. Detterman and Reed (1980) suggested that unmetamorphosed equivalents to these rocks may include both prearc sequences such as the Cottonwood Bay Greenstone and Kamishak Formation and synarc sequences such as the Talkeetna Formation.

The Cottonwood Bay Greenstone is a 600-m-thick sequence of metamorphosed mafic volcanic rocks. The volcanic sequence has been correlated with both Middle Norian (221–210 Ma; Wallace et al., 1989; R. Blodgett, 2004, personal commun.) rocks of the Tlikakila Complex (Wallace et al., 1989; Amato et al., this volume, chapter 10) and the Chilikadrotna Greenstone in the Lake Clark quadrangle (Nelson et al., 1983). The Cottonwood Bay basalts may be a western extension of the Nikolai Greenstone (Hillhouse, 1977; Nokleberg et al., 1994), an extensive Triassic

flood basalt that is exposed throughout the Wrangellia terrane in southern Alaska.

The Kamishak Formation overlies the Cottonwood Bay Greenstone and includes chert and limestone. The lower limestone units are interpreted as shallow marine sediments, and the chert is interpreted as having been deposited in a deep basin (Detterman and Reed, 1980). The rapid transition from shallow- to deep-water sedimentary rocks in exposures of the Kamishak Formation on the Alaska Peninsula is an example of a “drowning” event interpreted to be the result of a combination of sea level rise and tectonically driven subsidence (Wang et al., 1988). A multifraction zircon age of 200 ± 3 Ma from a tuff unit at the top of the section (Pálffy et al., 1999) and Norian fossils in limestones from the middle part of the Kamishak Formation (Detterman and Reed, 1980) are consistent with Late Triassic–Early Jurassic deposition.

The Tlikakila Complex in the Lake Clark quadrangle (Amato et al., this volume, chapter 10) includes greenschist facies metamorphic rocks with protoliths that include basalt, gabbro, ultramafic rocks, chert, mudstone, chert-pebble conglomerate, and minor quartz sandstone. These protoliths are inferred to be Triassic in age based on Norian fossils in limestone within the Chilikadrotna Greenstone in the Lake Clark region (Wallace et al., 1989). The metasedimentary rocks are likely correlative to the Kamishak Formation and the metasedimentary rocks in the Kakhonak Complex. The metabasic rocks in the Tlikakila Complex are likely correlative to the prearc Chilikadrotna Greenstone, Cottonwood Bay Greenstone, and Nikolai Greenstone. The volcanic rocks of the Tlikakila Complex are interpreted to have formed as a suprasubduction-zone ophiolite that was emplaced during the earliest part of the Talkeetna arc subduction system (Amato et al., this volume, chapter 10). Biotite $^{40}\text{Ar}/^{39}\text{Ar}$ ages from metasedimentary lithologies within the Tlikakila Complex record metamorphic cooling ages of 177 ± 1 Ma.

The Knik River Terrane (Pavlis, 1983; Pavlis et al., 1988) is a thin crustal sliver sandwiched between the Peninsular Terrane and the Chugach Terrane north of the Border Ranges fault (Pavlis, 1982; Little and Naeser, 1989). The terrane is divisible into two distinct assemblages based on lithology and cooling ages: a southern, metamorphic subterrane dominated by Cretaceous metamorphism and deformation, and a northern plutonic subterrane characterized by a predominance of Jurassic plutonic rocks with only scattered metamorphic screens. The metamorphic subterrane probably contains younger protoliths that postdate the Talkeetna arc (Pavlis et al., 1988), and thus, this assemblage has questionable affinities with the arc. Metamorphic screens within the plutonic subterrane, however, do contain direct information on the Talkeetna arc basement. These rocks consist of variably faulted greenschist–amphibolite facies metamorphic rocks. The assemblages are dominated by variably foliated greenschist and amphibolite derived from mafic protoliths interlayered quartzite, semipelitic schist, marble, and calc-schist (Pavlis, 1983). The protoliths are likely basalt flows with interbedded sedimentary rocks that were then deformed and metamorphosed together. These rocks are interpreted to be Triassic prearc basement to the Talkeetna arc (Pavlis, 1983; Pavlis et al., 1988).

Syn-Talkeetna Arc Volcanic and Plutonic Rocks

The Talkeetna Formation volcanic rocks (Detterman and Reed, 1980; Newberry et al., 1986; Clift et al., 2005a) preserve the volcanic carapace of the Talkeetna island arc (Burns, 1985; DeBari and Coleman, 1989). Fossils from within the Talkeetna Formation range from early Sinemurian to late Toarcian (202 ± 8 to 180 ± 8 Ma; 1999 GSA time scale; e.g., Grantz et al., 1963; Detterman and Hartssock, 1966; Gradstein and Ogg, 1996; Pálffy et al., 1999; Zhang and Blodgett, 2006). The Talkeetna Formation is bounded by Late Triassic and Bajocian units, providing a maximum period of arc volcanism from 206 ± 8 to 169 ± 8 Ma (1999 GSA time scale; e.g., Detterman and Hartssock, 1966; Detterman and Reed, 1980; Pálffy et al., 1999). These ages are consistent with three U-Pb zircon ages from the Alaska Peninsula that place the basal contact of the Talkeetna Formation between a $200.8 \pm 2.7/-2.8$ Ma tuff from the Kamishak Formation and $197.8 \pm 1.2/-0.4$ Ma and 197.8 ± 1.0 Ma tuffs from the lowest layers of the Talkeetna volcanic pile (Pálffy et al., 1999).

The Talkeetna arc plutonic rocks are in intrusive and faulted contact with the overlying Talkeetna Formation. Extensive U-Pb zircon dating indicates that these units show systematic age variations throughout the Peninsular Terrane (Roeske et al., 1989; Pálffy et al., 1999; Rioux et al., 2005, 2007). The oldest identified arc plutons are exposed north of the Border Ranges fault on Kodiak Island and yielded complex zircon U-Pb data suggesting an age of 217 ± 10 Ma (Roeske et al., 1989). Along strike to the east, more extensive exposures of plutonic rocks in the northern Chugach Mountains record crystallization ages from 202 to 181 Ma (Rioux et al., 2007). The locus of arc magmatism shifted northward at ca. 180 Ma, generating the large plutonic suites in the Talkeetna Mountains (177–154 Ma) and along the Alaska Peninsula (183–164 Ma). Evidence of inherited Paleozoic zircon in Early Jurassic plutons in the northwestern Talkeetna Mountains is consistent with assimilation of adjacent Wrangellia terrane crust into Wrangellian or Talkeetna arc plutons.

Isotopic analyses from Peninsular terrane rocks mirror the U-Pb systematics. Samarium-Nd and Rb-Sr isotopic analyses from Kodiak Island, the Chugach Mountains and the eastern Talkeetna Mountains yield a restricted range of isotopic ratios that are similar to modern intraoceanic settings (Rioux et al., 2007). In contrast, isotopic data from the western Talkeetna Mountains have more evolved ratios, consistent with the U-Pb zircon evidence for assimilation of Wrangellia crust. Isotopic ratios from the Alaska Peninsula overlap but are slightly more evolved than the arc-like ratios in the Chugach and eastern Talkeetna Mountains.

Postarc Assemblages

The Tuxedni Group (Detterman and Reed, 1980) directly overlies the Talkeetna Formation volcanic section along both faulted and unconformable contacts. The Tuxedni Group consists of marine units including graywacke, volcanic clast conglomerate, sandstone, and shale. Bajocian (ca. 176–169 Ma) ammonites from the Iliamna quadrangle are consistent with Middle Jurassic deposition (Detterman and Reed, 1980). The Chinitina (or Chinitna)

Formation overlies the Tuxedni Group and is a unit with marine siltstone and sandstone of Callovian age (164–159 Ma; Gradstein and Ogg, 1996; Detterman and Reed, 1980; Trop et al., 2005).

PETROLOGY OF THE DATED SAMPLES

Samples for dating were collected from the following formations: (1) low-grade metamorphosed sandstone and metavolcanic rocks from the Kakhonak Complex, (2) sandstones from the Talkeetna Formation in the Katmai and Iliamna quadrangles, (3) greenschist-facies metabasalt from the Chugach Mountains, and (4) Middle Jurassic sandstones overlying the Talkeetna Formation in the Little Oshetna Valley of the Talkeetna Mountains. Brief petrologic descriptions of these samples follow.

Kakhonak Complex

Three samples were collected from the Kakhonak Complex. Sample 2728-M06 (Fig. 2) is a low-grade, medium- to coarse-grained metasediment from exposures of metamorphic rocks near Naknek Lake in the Iliamna quadrangle. The sample contains ~50% quartz, 30% plagioclase, and 20% chlorite + recrystallized volcanic lithic grains. No foliation was observed. Quartz grains are rounded and up to 3 mm in diameter. Lithic grains are 5–10 mm in diameter. Plagioclase grains are 1–3 mm in diameter.

Sample 2728-M05 (Fig. 2) is from an island in Naknek Lake in the Iliamna quadrangle. The sample is a metamorphosed volcanic or volcanoclastic rock with a foliation defined by quartz, plagioclase, and varying proportions of Fe-Ti oxides. The rock is very fine-grained and contains ~70% quartz, 25% plagioclase, and 5% Fe-Ti oxides. White mica, titanite, tourmaline, and zircon are present in trace amounts. Quartz and plagioclase are equant and ~50 μ m in diameter, although coarser grains of plagioclase and quartz (~1 mm across) are also present as less than 5% of the total volume of the rock. There are no lithic grains present. A <1-cm-thick granitic dikelet cuts this rock and is concordant to the foliation.

Sample 2731-P02 (Fig. 2) was collected from a thin exposure of the Kakhonak Complex east of Chinitna Bay in the northwest Iliamna quadrangle. It consists of cryptocrystalline quartz with relict grain boundaries surrounding optically continuous aggregates of small grains. The protolith is unknown but likely sedimentary.

Western Chugach Mountains/Knik River Terrane

A single sample of greenschist facies metabasalt was collected from the western Chugach Mountains just north of the Border Ranges fault zone. Sample 2709-B08 (Fig. 3) has a strong foliation and consists of pleochroic green amphibole, probably tremolite-actinolite, chlorite, plagioclase, and quartz. The sample is cut by quartz veins with grains flattened parallel to the foliation.

Talkeetna Formation

One sample was collected from within the Talkeetna Formation in the Johnson River drainage of the westernmost Kenai

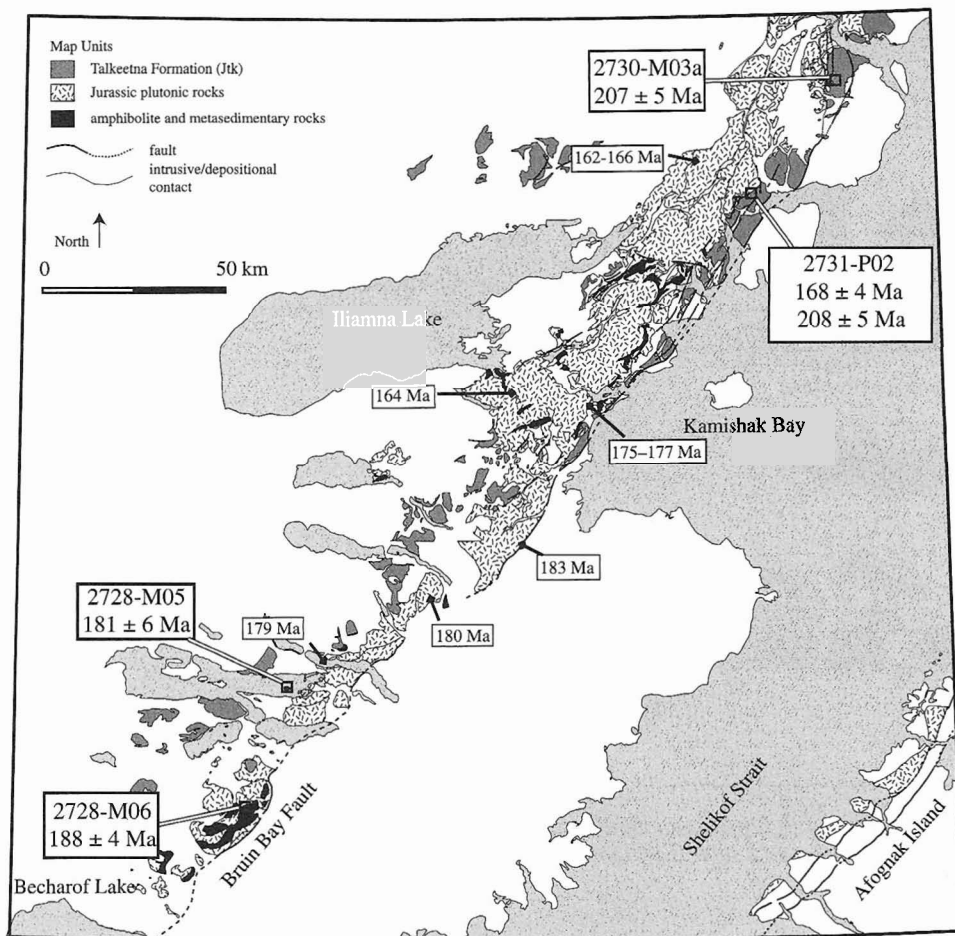


Figure 2. Simplified geologic map of the Alaska Peninsula region showing sample locations. Ages in small boxes are from Rioux et al. (2005). Ages in large boxes are from this study. Modified from Detterman et al. (1976; Kenai), Connelly and Moore (1979; Kodiak), Detterman and Reed (1980; Iliamna), Nelson et al. (1983; Lake Clark), Riehle et al. (1993; Katmai), Bradley et al. (1999; Seldovia).

quadrangle. Sample 2730-M03a (Fig. 2) is a volcanic breccia with basalt lithic clasts, plagioclase and resorbed quartz phenocrysts, angular glass shards, and a glassy matrix. It was collected from the base of a fossiliferous limestone sequence at the base of the Talkeetna Formation.

Tuxedni Group/Chinitna Formation

A sample of volcanoclastic sandstone, 3626-C01 (Fig. 3), was collected from the base of the Chinitna Formation immediately overlying the uppermost lavas of the Talkeetna Formation in the Little Oshetna Valley (see Figure 5 in Clift et al., 2005a). In this area, the Talkeetna Formation is unconformably overlain by the Chinitna Formation and Tuxedni Group (Trop et al., 2005), whereas correlative rocks on the Alaska Peninsula are simply assigned to the Tuxedni Group (Detterman and Reed, 1980).

U-Pb GEOCHRONOLOGY

Analytical Techniques

Approximately 2–5 kg of sample were crushed, sieved to <300 μm , and processed for mineral separations. Zircons were

concentrated using lithium metatungstate, magnetic separation, and lastly methylene iodide (MEI). All material that sank in MEI was put on 2.5 cm epoxy mounts for analysis. Zircon yields were generally low owing to relatively small sample sizes, and in most cases all available zircons were analyzed.

Uranium-lead zircon analyses were conducted by laser-ablation multicollector inductively coupled plasma mass spectrometry (LA-MC-ICP-MS) at the University of Arizona. Samples were analyzed in two sessions in May (2728-M05, 2728-M06, 2730-M03a, and 2731-P02) and November (2709-B08 and 3626-C01) 2003. Individual spot analyses were carried out using a New Wave DUV193 Excimer laser (operating at a wavelength of 193 nm) with spot diameters of 25 μm (Samples 2728-M06 and 2731-P02), 35 μm (Samples 2730-M03a and 2728-M05) and 50 μm (Samples 3626-C01 and 2709-B08). If the location of the analysis is not specified in the text or table, the core of the grain was analyzed.

The ablated material was transported in an Ar-He carrier gas into the plasma source of a Micromass Isoprobe, which is equipped with a flight tube of sufficient width to allow simultaneous analysis of U, Th, and Pb isotopes. All measurements were made in static mode, using Faraday detectors for ^{238}U , ^{232}Th , $^{208-206}\text{Pb}$ and an ion-counting channel for ^{204}Pb . Ion yields were ~ 1 mv per ppm.

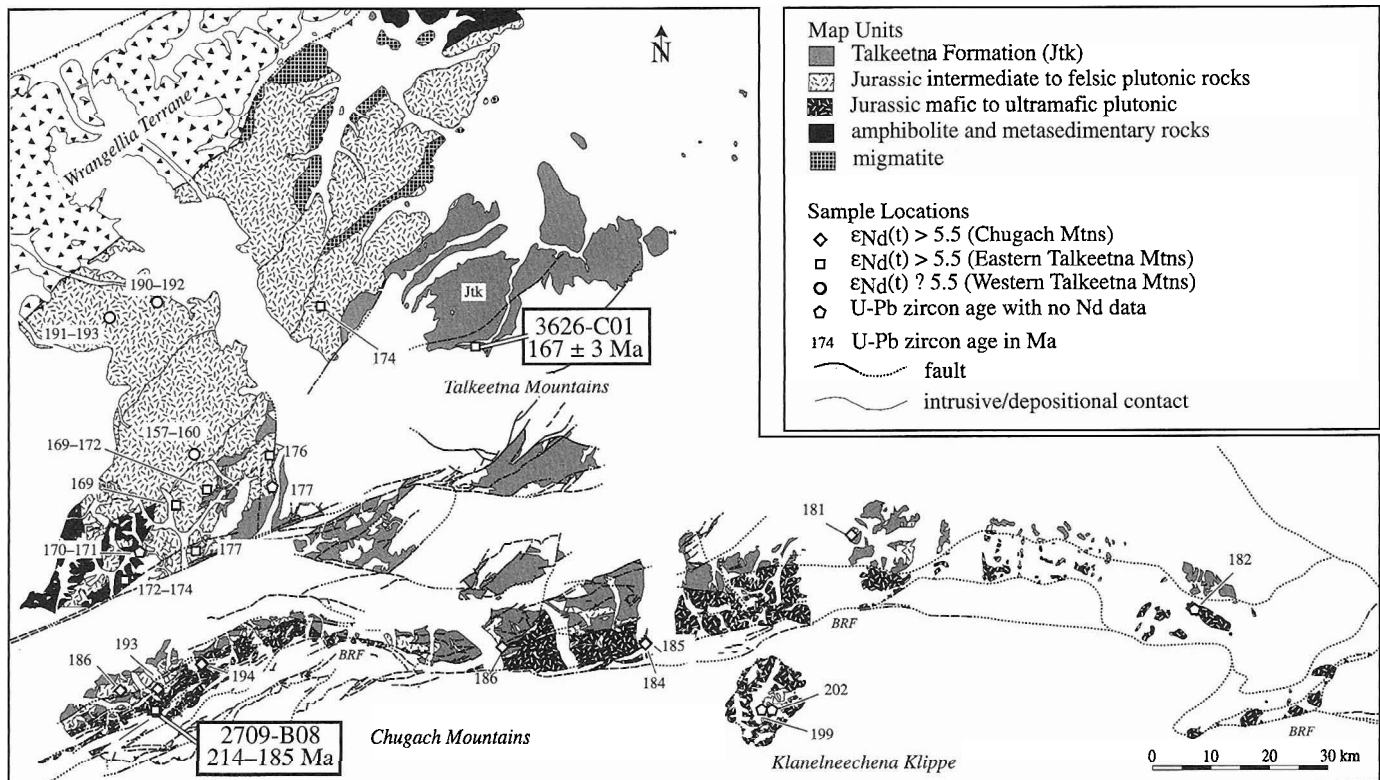


Figure 3. Simplified geologic map of the Chugach/Talkeetna Mountains area showing sample locations. Ages in small boxes are from Rioux et al. (2007). Ages in large boxes are from this study. BRF is the Border Ranges fault. Geology modified after Csejtey et al. (1978), Winkler et al. (1981), Winkler (1992), and Wilson et al. (1998).

Each analysis consisted of an integrated 20-second background measurement on the peak positions, 20 1-second integrations with the laser firing, and a 30-second delay to purge the previous sample and prepare for the next analysis. The ablation pits were $\sim 20 \mu\text{m}$ in depth.

Common Pb corrections were made using measured ^{204}Pb concentrations and assuming an initial Pb composition from Stacey and Kramers (1975) with uncertainties of 1.0 for $^{206}\text{Pb}/^{204}\text{Pb}$ and 0.3 for $^{207}\text{Pb}/^{204}\text{Pb}$. Prior analyses have demonstrated that the Ar-He carrier gas contains negligible ^{204}Hg , and we corrected for isobaric ^{204}Hg interferences on ^{204}Pb as part of the background measurements.

Element and isotopic fractionation for LA-ICP-MS vary with pit depth, and the accepted isotope ratios were determined by least-squares projection through the measured values back to the initial determination. Interelement fractionation of Pb/U was generally $<20\%$, whereas fractionation of Pb isotopes was generally $<5\%$. Each analysis was normalized to the University of Arizona "SL" zircon standard with an age of $564 \pm 4 \text{ Ma}$ (G. Gehrels, 2005, personal commun.), which was analyzed after every fifth sample analysis. The uncertainty resulting from the calibration correction (together with the uncertainty from decay constants and common Pb composition) is generally 3% (2σ) for $^{206}\text{Pb}/^{238}\text{U}$ and $^{207}\text{Pb}/^{206}\text{Pb}$ ages of $>1.2 \text{ Ga}$.

The measured isotopic ratios and ages are reported in Table 1. Errors from the measurement of $^{206}\text{Pb}/^{238}\text{U}$, $^{206}\text{Pb}/^{207}\text{Pb}$, and $^{206}\text{Pb}/^{204}\text{Pb}$ are reported at the 1-sigma level. Additional errors that affect all ages include uncertainties from (1) U decay constants; (2) the composition of common Pb; and (3) calibration correction. These systematic errors are not included in Table 1 and add an additional 1.8%–2% (2σ) uncertainty to $^{206}\text{Pb}/^{238}\text{U}$ and older $^{207}\text{Pb}/^{206}\text{Pb}$ ages. Interpreted ages incorporate the systematic errors and are cited at the 2σ level.

Ages used for interpretation are $^{206}\text{Pb}/^{238}\text{U}$ ages for grains $<800 \text{ Ma}$ and $^{207}\text{Pb}/^{206}\text{Pb}$ ages for grains $>800 \text{ Ma}$. Analyses with $>10\%$ 1σ uncertainty, $>30\%$ normal discordance, or $>5\%$ reverse discordance are excluded from the plots and interpretations. Relative probability diagrams and weighted mean calculations were created using the Isoplot program (Ludwig, 2002). For other details of analytical methods see Barbeau et al. (2005).

Geochronology Results

Kakhonak Complex

Forty-six zircons were analyzed from sample 2728-M06 (Fig. 4). Zircon grain lengths range from 50 to 200 μm . Most grains were subhedral to euhedral and ranged from small equant

TABLE 1. U-Pb ZIRCON GEOCHRONOLOGIC ANALYSES BY LASER-ABLATION MULTICOLLECTOR ICP MASS SPECTROMETRY

	Isotopic ratios								Apparent ages (Ma)							
	U (ppm)	$\frac{^{206}\text{Pb}_m}{^{204}\text{Pb}}$	U/Th	$\frac{^{207}\text{Pb}^*}{^{235}\text{U}}$	\pm (%)	$\frac{^{206}\text{Pb}^*}{^{238}\text{U}}$	\pm (%)	error corr.	$\frac{^{206}\text{Pb}^*}{^{238}\text{U}}$	\pm (Ma)	$\frac{^{207}\text{Pb}^*}{^{235}\text{U}}$	\pm (Ma)	$\frac{^{206}\text{Pb}^*}{^{207}\text{Pb}^*}$	\pm (Ma)	Age	\pm (Ma) 1 σ
2728-M06-1	31	663	3	0.07531	34.92	0.01248	2.11	0.06	80.0	1.7	74	26		80.0	1.7	
2728-M06-2	33	768	2	0.07472	17.61	0.01307	1.54	0.09	83.7	1.3	73	13		83.7	1.3	
2728-M06-3	13	1647	11	0.09103	20.46	0.01392	4.49	0.22	89.1	4.0	89	19		89.1	4.0	
2728-M06-4	7	6243	123	0.11453	16.73	0.01480	9.24	0.55	94.7	8.8	110	19		94.7	8.8	
2728-M06-5	59	6715	11	0.11119	38.31	0.01506	4.55	0.12	96.4	4.4	107	42		96.4	4.4	
2728-M06-6	25	1130	3	0.07834	35.19	0.01544	5.76	0.16	98.7	5.7	77	28		98.7	5.7	
2728-M06-7	17	1784	6	0.10730	5.25	0.01571	3.46	0.66	100.5	3.5	104	6		100.5	3.5	
2728-M06-8	39	5204	6	0.17526	33.94	0.02585	6.57	0.19	164.5	10.9	164	59		164.5	10.9	
2728-M06-9	11	629	11	0.18157	19.67	0.02606	5.41	0.28	165.9	9.1	169	36		165.9	9.1	
2728-M06-10	49	14547	9	0.16855	14.40	0.02727	4.32	0.30	173.5	7.6	158	24		173.5	7.6	
2728-M06-11	65	10710	7	0.18741	10.05	0.02807	3.01	0.30	178.4	5.4	174	19		178.4	5.4	
2728-M06-12	14	3283	14	0.22211	40.77	0.02875	2.66	0.07	182.7	4.9	204	88		182.7	4.9	
2728-M06-13	25	5307	7	0.19999	15.47	0.02918	2.04	0.13	185.4	3.8	185	31		185.4	3.8	
2728-M06-14	51	7792	8	0.19355	16.23	0.02936	3.02	0.19	186.6	5.7	180	31		186.6	5.7	
2728-M06-15	73	16814	6	0.20450	5.56	0.02938	0.82	0.15	186.7	1.6	189	12		186.7	1.6	
2728-M06-16	17	7333	11	0.20672	22.83	0.02956	2.01	0.09	187.8	3.8	191	47		187.8	3.8	
2728-M06-17	93	53169	7	0.21402	8.38	0.02958	0.85	0.10	187.9	1.6	197	18		187.9	1.6	
2728-M06-18	40	19335	7	0.21369	11.28	0.02983	1.34	0.12	189.5	2.6	197	24		189.5	2.6	
2728-M06-19	11	2123	16	0.20902	32.49	0.02993	3.66	0.11	190.1	7.1	193	67		190.1	7.1	
2728-M06-20	23	7184	8	0.18560	25.77	0.03001	1.76	0.07	190.6	3.4	173	47		190.6	3.4	
2728-M06-21	51	683755	8	0.22430	7.19	0.03008	1.22	0.17	191.0	2.4	206	16		191.0	2.4	
2728-M06-22	19	6052	12	0.17453	60.78	0.03013	1.52	0.03	191.3	3.0	163	102		191.3	3.0	
2728-M06-23	58	11276	6	0.19988	8.25	0.03012	1.20	0.15	191.3	2.3	185	17		191.3	2.3	
2728-M06-24	7	1599	12	0.20184	43.31	0.03044	9.99	0.23	193.3	19.6	187	85		193.3	19.6	
2728-M06-25	45	552801	11	0.21248	7.00	0.03045	1.61	0.23	193.3	3.2	196	15		193.3	3.2	
2728-M06-26	63	21562	8	0.19099	12.36	0.03063	0.74	0.06	194.5	1.5	178	24		194.5	1.5	
2728-M06-27	121	96842	8	0.22567	4.05	0.03081	1.32	0.33	195.6	2.6	207	9		195.6	2.6	
2728-M06-28	91	23791	7	0.20377	7.66	0.03084	1.52	0.20	195.8	3.0	188	16		195.8	3.0	
2728-M06-29	32	13668	9	0.22589	22.22	0.03121	1.01	0.05	198.1	2.0	207	50		198.1	2.0	
2728-M06-30	49	11691	7	0.20532	6.77	0.03140	1.29	0.19	199.3	2.6	190	14		199.3	2.6	
2728-M06-31	33	36481	7	0.21745	14.65	0.03171	1.00	0.07	201.2	2.0	200	32		201.2	2.0	
2728-M06-32	24	12810	10	0.20568	15.42	0.03208	1.22	0.08	203.5	2.5	190	32		203.5	2.5	
2728-M06-33	12	2727	7	0.19674	40.79	0.03239	3.37	0.08	205.5	7.0	182	78		205.5	7.0	
2728-M06-34	15	3309	18	0.24825	39.11	0.03239	1.76	0.05	205.5	3.7	225	94		205.5	3.7	
2728-M06-35	27	15487	14	0.24830	17.81	0.03249	0.80	0.05	206.1	1.7	225	44		206.1	1.7	
2728-M06-36	63	111689	7	0.23684	5.70	0.03312	1.11	0.20	210.1	2.4	216	14		210.1	2.4	
2728-M06-37	49	3334	3	0.24527	3.05	0.03447	2.16	0.71	218.4	4.8	223	8		218.4	4.8	
2728-M06-38	14	1377	15	0.22679	12.53	0.03448	1.67	0.13	218.5	3.7	208	29		218.5	3.7	
2728-M06-39	41	13387	8	0.29455	7.54	0.04083	1.28	0.17	258.0	3.4	262	22		258.0	3.4	

(continued)

TABLE 1. U-Pb ZIRCON GEOCHRONOLOGIC ANALYSES BY LASER-ABLATION MULTICOLLECTOR ICP MASS SPECTROMETRY (continued)

	Isotopic ratios								Apparent ages (Ma)							
	U (ppm)	$\frac{^{206}\text{Pb}_m}{^{204}\text{Pb}}$	U/Th	$\frac{^{207}\text{Pb}^*}{^{235}\text{U}}$	\pm (%)	$\frac{^{206}\text{Pb}^*}{^{238}\text{U}}$	\pm (%)	error corr.	$\frac{^{206}\text{Pb}^*}{^{238}\text{U}}$	\pm (Ma)	$\frac{^{207}\text{Pb}^*}{^{235}\text{U}}$	\pm (Ma)	$\frac{^{206}\text{Pb}^*}{^{207}\text{Pb}^*}$	\pm (Ma)	Age	\pm (Ma) 1 σ
2728-M06-40	23	4258	7	0.50590	9.78	0.06577	3.19	0.33	410.6	13.5	416	49			410.6	13.5
2728-M06-41	24	36725	16	0.95572	4.38	0.10604	0.61	0.14	649.7	4.2	681	42			649.7	4.2
2728-M06-42	97	79597	38	0.92169	1.44	0.10659	0.96	0.67	652.9	6.6	663	13			652.9	6.6
2728-M06-43	2	7066	281	0.88154	29.84	0.11421	4.44	0.15	697.2	32.6	642	237			697.2	32.6
2728-M06-44	2	318	22	1.39669	18.48	0.12743	9.21	0.50	773.2	75.2	888	233			773.2	75.2
2728-M06-45	15	409651	11	3.39317	3.19	0.26125	2.97	0.93	1496.2	49.8	1503	104	1512	11	1512.0	11.0
2728-M06-46	94	210208	14	3.22813	1.30	0.24194	1.25	0.96	1396.8	19.4	1464	42	1563	3	1563.0	3.0
2728-M05-1	37	1152	5	0.07856	15.48	0.01312	1.65	0.11	84.0	1.4	77	12			84.0	1.4
2728-M05-2	3	711	26	0.13888	22.56	0.02596	8.05	0.36	165.2	13.5	132	31			165.2	13.5
2728-M05-3	26	2586	47	0.21132	18.74	0.02621	2.88	0.15	166.8	4.9	195	39			166.8	4.9
2728-M05-4	8	1006	4	0.17788	88.04	0.02662	8.53	0.10	169.4	14.6	166	148			169.4	14.6
2728-M05-5	21	2664	143	0.16932	31.01	0.02746	3.05	0.10	174.6	5.4	159	52			174.6	5.4
2728-M05-6	8	860	2	0.20621	23.28	0.02795	4.40	0.19	177.7	7.9	190	48			177.7	7.9
2728-M05-7	10	1070	43	0.20233	19.41	0.02861	2.88	0.15	181.8	5.3	187	39			181.8	5.3
2728-M05-8	14	2909	13	0.27724	33.52	0.02866	2.14	0.06	182.2	4.0	249	90			182.2	4.0
2728-M05-9	6	973	5	0.14687	62.47	0.02909	3.95	0.06	184.8	7.4	139	89			184.8	7.4
2728-M05-10	17	2390	23	0.17677	13.89	0.02917	3.81	0.27	185.4	7.2	165	25			185.4	7.2
2728-M05-11	8	1366	256	0.17884	29.54	0.02920	2.33	0.08	185.5	4.4	167	52			185.5	4.4
2728-M05-12	11	1761	3	0.27907	23.04	0.02959	2.90	0.13	188.0	5.5	250	63			188.0	5.5
2728-M05-13	7	1744	58	0.22915	164.65	0.03000	3.56	0.02	190.6	6.9	210	325			190.6	6.9
2728-M05-14	4	1623	2	0.26117	124.31	0.03031	7.51	0.06	192.5	14.7	236	286			192.5	14.7
2728-M05-15	9	953	104	0.19666	13.75	0.03187	5.16	0.38	202.2	10.6	182	27			202.2	10.6
2728-M05-16	12	2265	4	0.22929	37.96	0.03406	2.41	0.06	215.9	5.3	210	85			215.9	5.3
2728-M05-17	2	1181	54	0.31214	18.10	0.03482	11.13	0.62	220.7	24.9	276	56			220.7	24.9
2728-M05-18	2	866	4	0.23784	34.57	0.03563	16.02	0.46	225.7	36.7	217	80			225.7	36.7
2728-M05-19	4	772	5	0.25176	15.60	0.03915	6.70	0.43	247.5	16.9	228	39			247.5	16.9
2728-M05-20	11	1508	1	0.28100	24.61	0.04742	8.76	0.36	298.7	26.7	252	68			298.7	26.7
2728-M05-21	6	810	30	0.40924	65.91	0.05335	5.31	0.08	335.1	18.2	348	243			335.1	18.2
2728-M05-22	1	1997	18	0.69274	26.16	0.09202	9.58	0.37	567.5	56.6	534	169			567.5	56.6
2728-M05-23	15	59689	7	3.18433	1.86	0.24959	0.72	0.39	1436.3	11.6	1453	58	1478	16	1478.0	16.0
2728-M05-24	59	5394	37	4.30123	8.17	0.28501	3.71	0.46	1616.5	67.9	1694	306	1790	66	1790.0	66.0
2728-M05-25	30	919069	11	12.51144	1.13	0.50889	1.11	0.99	2651.9	36.3	2644	134	2637	2	2637.0	2.0
2731-P02-1	8	978	56	0.17434	51.68	0.02269	3.94	0.08	144.6	5.8	163	88			144.6	5.8
2731-P02-2	6	1131	180	0.17869	119.17	0.02405	10.08	0.09	153.2	15.6	167	196			153.2	15.6
2731-P02-3	7	1030	90	0.16202	33.54	0.02463	4.62	0.14	156.8	7.3	153	54			156.8	7.3
2731-P02-4	8	1193	79	0.17541	84.40	0.02556	4.24	0.05	162.7	7.0	164	140			162.7	7.0
2731-P02-5	5	1233	140	0.18092	37.24	0.02627	4.71	0.13	167.2	8.0	169	66			167.2	8.0

(continued)

TABLE 1. U-Pb ZIRCON GEOCHRONOLOGIC ANALYSES BY LASER-ABLATION MULTICOLLECTOR ICP MASS SPECTROMETRY (continued)

	Isotopic ratios								Apparent ages (Ma)						
	U (ppm)	$\frac{^{206}\text{Pb}_m}{^{204}\text{Pb}}$	U/Th	$\frac{^{207}\text{Pb}^*}{^{235}\text{U}}$	\pm (%)	$\frac{^{206}\text{Pb}^*}{^{238}\text{U}}$	\pm (%)	error corr.	$\frac{^{206}\text{Pb}^*}{^{238}\text{U}}$	\pm (Ma)	$\frac{^{207}\text{Pb}^*}{^{235}\text{U}}$	\pm (Ma)	$\frac{^{206}\text{Pb}^*}{^{207}\text{Pb}^*}$	\pm (Ma)	Age
2731-P02-6	8	736	92	0.15774	325.31	0.02630	7.26	0.02	167.4	12.3	149	421		167.4	12.3
2731-P02-7	5	1230	92	0.18391	87.46	0.02641	5.73	0.07	168.0	9.7	171	151		168.0	9.7
2731-P02-8	16	1553	44	0.19974	33.51	0.02652	1.50	0.05	168.7	2.6	185	66		168.7	2.6
2731-P02-9	5	998	25	0.14197	52.81	0.02673	9.21	0.17	170.1	15.8	135	73		170.1	15.8
2731-P02-10	3	958	44	0.19714	58.43	0.02725	7.63	0.13	173.3	13.4	183	111		173.3	13.4
2731-P02-11	6	1074	62	0.19187	114.63	0.02929	5.54	0.05	186.1	10.4	178	202		186.1	10.4
2731-P02-12	13	2547	124	0.17995	8.99	0.02961	2.73	0.30	188.1	5.2	168	16		188.1	5.2
2731-P02-13	215	1757	8681	0.19986	6.46	0.03211	6.00	0.93	203.7	12.4	185	13		203.7	12.4
2731-P02-14	15	751	3532	0.16848	13.00	0.03216	2.59	0.20	204.0	5.4	158	22		204.0	5.4
2731-P02-15	6	2742	147	0.21025	35.45	0.03247	3.50	0.10	206.0	7.3	194	73		206.0	7.3
2731-P02-16	32	2581	2240	0.22045	11.47	0.03266	6.06	0.53	207.2	12.8	202	25		207.2	12.8
2731-P02-17	17	7199	19	0.24123	14.05	0.03286	2.19	0.16	208.4	4.6	219	34		208.4	4.6
2731-P02-18	11	661	303	0.15479	20.73	0.03395	4.67	0.23	215.2	10.2	146	32		215.2	10.2
2731-P02-19	6	839	179	0.17546	24.11	0.03430	3.93	0.16	217.4	8.7	164	42		217.4	8.7
2731-P02-20	14	3233	12	0.24958	21.15	0.03541	1.42	0.07	224.3	3.2	226	52		224.3	3.2
2731-P02-21	83	4755	9	0.26404	5.31	0.03878	2.05	0.39	245.3	5.1	238	14		245.3	5.1
2731-P02-22	4	1297	5349	0.30926	14.16	0.05373	4.34	0.31	337.4	15.0	274	44		337.4	15.0
2731-P02-23	5	1528	1876	0.43231	14.70	0.06142	9.10	0.62	384.2	35.9	365	63		384.2	35.9
2731-P02-24	6	1677	3626	0.37314	6.65	0.06531	4.80	0.72	407.8	20.2	322	25		407.8	20.2
2731-P02-25	13	17067	38	0.58085	22.30	0.07888	1.62	0.07	489.5	8.3	465	124		489.5	8.3
2731-P02-26	14	13398	6	0.56861	18.40	0.08500	1.16	0.06	525.9	6.3	457	101		525.9	6.3
2731-P02-27	11	15306	23	0.51418	11.35	0.08558	1.28	0.11	529.3	7.1	421	58		529.3	7.1
2731-P02-28	24	3177	23	0.67333	4.73	0.09921	0.55	0.12	609.8	3.5	523	32		609.8	3.5
2731-P02-29	18	2640	22	0.67889	8.59	0.10043	0.96	0.11	616.9	6.2	526	58		616.9	6.2
2709-B08-2r	2520	30855	6.3	0.21557	1.20	0.03211	0.56	0.47	203.8	1.2	198.2	2.6		203.8	1.2
2709-B08-3r	620	5175	7.1	0.20936	6.53	0.03136	0.35	0.05	199.0	0.7	193.0	13.8		199.0	0.7
2709-B08-4c	786	18576	7.6	0.22400	1.99	0.03092	0.60	0.30	196.3	1.2	205.2	4.5		196.3	1.2
2709-B08-5c	173	3741	10.5	0.20798	15.20	0.03167	0.59	0.04	201.0	1.2	191.9	31.6		201.0	1.2
2709-B08-6c	126	4176	8.1	0.13501	19.99	0.03071	0.84	0.04	195.0	1.7	128.6	27.0		195.0	1.7
2709-B08-7c	1664	1497	11.6	0.17748	16.60	0.03080	0.25	0.02	195.6	0.5	165.9	29.5		195.6	0.5
2709-B08-8c	1360	315	20.8	0.01312	88.89	0.02917	0.41	0.00	185.3	0.8	13.2	11.8		185.3	0.8
2709-B08-9c	192	2172	7.4	0.19049	19.74	0.03126	0.87	0.04	198.4	1.8	177.0	37.5		198.4	1.8
2709-B08-9c	634	7815	8.9	0.20520	5.06	0.03071	0.27	0.05	195.0	0.5	189.5	10.5		195.0	0.5
2709-B08-10c	634	7815	8.9	0.20520	5.06	0.03071	0.27	0.05	195.0	0.5	189.5	10.5		195.0	0.5
2709-B08-11c	136	3312	8.6	0.18245	24.16	0.03189	1.81	0.07	202.3	3.7	170.2	43.8		202.3	3.7
2709-B08-12c	171	3495	9.4	0.27133	7.71	0.03186	0.42	0.05	202.2	0.9	243.8	21.0		202.2	0.9
2709-B08-13c	146	1305	7.2	0.16720	20.17	0.03092	0.90	0.04	196.3	1.8	157.0	33.7		196.3	1.8
2709-B08-14c	118	852	10.2	0.17227	28.38	0.03081	0.36	0.01	195.6	0.7	161.4	48.5		195.6	0.7

(continued)

TABLE 1. U-Pb ZIRCON GEOCHRONOLOGIC ANALYSES BY LASER-ABLATION MULTICOLLECTOR ICP MASS SPECTROMETRY (continued)

	Isotopic ratios								Apparent ages (Ma)							
	U (ppm)	$\frac{^{206}\text{Pb}_m}{^{204}\text{Pb}}$	U/Th	$\frac{^{207}\text{Pb}^*}{^{235}\text{U}}$	\pm (%)	$\frac{^{206}\text{Pb}^*}{^{238}\text{U}}$	\pm (%)	error corr.	$\frac{^{206}\text{Pb}^*}{^{238}\text{U}}$	\pm (Ma)	$\frac{^{207}\text{Pb}^*}{^{235}\text{U}}$	\pm (Ma)	$\frac{^{206}\text{Pb}^*}{^{207}\text{Pb}^*}$	\pm (Ma)	Age	\pm (Ma) 1σ
2709-B08-15c	369	1722	5.1	0.16554	16.60	0.03149	0.70	0.04	199.8	1.4	155.5	27.5		199.8	1.4	
2709-B08-16c	1088	18837	4.7	0.21727	2.11	0.03198	0.73	0.35	202.9	1.5	199.6	4.6		202.9	1.5	
2709-B08-17c	220	3510	6.0	0.15819	13.54	0.03018	1.14	0.08	191.7	2.2	149.1	21.5		191.7	2.2	
2709-B08-18c	288	6804	7.0	0.24498	6.65	0.03090	0.62	0.09	196.2	1.2	222.5	16.4		196.2	1.2	
2709-B08-19c	151	2496	10.8	0.21813	18.87	0.03143	0.94	0.05	199.5	1.9	200.4	40.9		199.5	1.9	
2709-B08-20c	159	3972	6.7	0.18166	15.13	0.03143	0.60	0.04	199.5	1.2	169.5	27.5		199.5	1.2	
2709-B08-21c	115	2178	13.3	0.19870	16.93	0.03218	0.99	0.06	204.2	2.1	184.0	33.6		204.2	2.1	
2709-B08-22c	167	3153	8.2	0.19750	16.26	0.03189	0.63	0.04	202.4	1.3	183.0	32.1		202.4	1.3	
2709-B08-23c	343	9354	7.7	0.23761	5.73	0.03154	0.31	0.05	200.2	0.6	216.5	13.7		200.2	0.6	
2709-B08-24c	226	6654	7.5	0.15569	10.48	0.03113	0.54	0.05	197.6	1.1	146.9	16.4		197.6	1.1	
2709-B08-25c	115	2697	11.7	0.19632	26.33	0.03036	1.04	0.04	192.8	2.0	182.0	51.2		192.8	2.0	
2709-B08-26c	127	2454	5.5	0.26177	11.91	0.03140	2.36	0.20	199.3	4.8	236.1	31.2		199.3	4.8	
2709-B08-27c	115	1731	8.5	0.16047	21.06	0.03049	1.16	0.06	193.6	2.3	151.1	33.7		193.6	2.3	
2709-B08-28c	2090	26007	10.2	0.21596	1.37	0.03174	0.56	0.41	201.4	1.1	198.5	3.0		201.4	1.1	
2709-B08-29c	194	2139	5.6	0.23410	12.63	0.03171	0.93	0.07	201.3	1.9	213.6	29.6		201.3	1.9	
2709-B08-30c	392	11877	6.6	0.21500	5.55	0.03244	0.28	0.05	205.8	0.6	197.7	12.0		205.8	0.6	
2709-B08-31c	272	5121	9.6	0.20274	8.49	0.03227	0.68	0.08	204.7	1.4	187.4	17.3		204.7	1.4	
2709-B08-32c	187	4896	11.6	0.18281	10.95	0.03150	1.01	0.09	199.9	2.1	170.5	20.1		199.9	2.1	
2709-B08-33c	212	405	2.7	0.07641	57.22	0.03367	0.48	0.01	213.5	1.1	74.8	43.4		213.5	1.1	
2709-B08-34c	2096	17061	3.7	0.21779	1.85	0.03143	0.46	0.25	199.5	0.9	200.1	4.1		199.5	0.9	
2709-B08-35c	73	1578	6.2	0.27639	26.85	0.03119	1.21	0.05	198.0	2.4	247.8	72.7		198.0	2.4	
2709-B08-04r	2318	21348	6.4	0.20398	2.06	0.02948	1.07	0.52	187.3	2.0	188.5	4.3		187.3	2.0	
2709-B08-05r	275	4077	11.7	0.20599	9.45	0.03011	1.35	0.14	191.2	2.6	190.2	19.6		191.2	2.6	
2709-B08-07r	2616	1173	8.3	0.15416	21.13	0.02961	0.58	0.03	188.1	1.1	145.6	32.6		188.1	1.1	
2730-M03a-1	13	3200	10	0.18364	22.13	0.02894	3.26	0.15	183.9	6.1	171	41		183.9	6.1	
2730-M03a-2	5	2424	10	0.22402	102.02	0.02972	3.61	0.04	188.8	6.9	205	209		188.8	6.9	
2730-M03a-3	8	1389	19	0.22542	57.37	0.03021	2.50	0.04	191.9	4.9	206	124		191.9	4.9	
2730-M03a-4	44	2398	6	0.19165	12.77	0.03026	7.11	0.56	192.2	13.9	178	25		192.2	13.9	
2730-M03a-5	13	2691	15	0.24387	29.45	0.03070	2.27	0.08	194.9	4.5	222	70		194.9	4.5	
2730-M03a-6	18	2070	9	0.18698	27.01	0.03083	1.58	0.06	195.7	3.1	174	50		195.7	3.1	
2730-M03a-7	12	2932	10	0.30142	35.39	0.03134	2.15	0.06	199.0	4.3	268	103		199.0	4.3	
2730-M03a-8	10	1748	13	0.28723	41.47	0.03147	1.99	0.05	199.8	4.0	256	114		199.8	4.0	
2730-M03a-9	9	2998	26	0.23664	17.45	0.03168	2.86	0.16	201.0	5.8	216	41		201.0	5.8	
2730-M03a-10	10	2242	19	0.20555	27.38	0.03169	2.08	0.08	201.1	4.3	190	56		201.1	4.3	
2730-M03a-11	11	4067	21	0.22081	28.04	0.03169	2.43	0.09	201.1	5.0	203	61		201.1	5.0	
2730-M03a-12	12	1157	19	0.19808	21.90	0.03173	2.03	0.09	201.4	4.1	184	43		201.4	4.1	
2730-M03a-13	9	2095	10	0.24024	23.94	0.03184	2.27	0.10	202.0	4.7	219	57		202.0	4.7	
2730-M03a-14	14	2725	12	0.22718	22.99	0.03189	2.96	0.13	202.3	6.1	208	52		202.3	6.1	

(continued)

TABLE 1. U-Pb ZIRCON GEOCHRONOLOGIC ANALYSES BY LASER-ABLATION MULTICollector ICP MASS SPECTROMETRY (continued)

	Isotopic ratios								Apparent ages (Ma)							
	U (ppm)	$\frac{^{206}\text{Pb}_m}{^{204}\text{Pb}}$	U/Th	$\frac{^{207}\text{Pb}^*}{^{235}\text{U}}$	± (%)	$\frac{^{206}\text{Pb}^*}{^{238}\text{U}}$	± (%)	error corr.	$\frac{^{206}\text{Pb}^*}{^{238}\text{U}}$	± (Ma)	$\frac{^{207}\text{Pb}^*}{^{235}\text{U}}$	± (Ma)	$\frac{^{206}\text{Pb}^*}{^{207}\text{Pb}^*}$	± (Ma)	Age	± (Ma) 1σ
2730-M03a-15	10	1724	13	0.19660	64.20	0.03193	1.96	0.03	202.6	4.0	182	121		202.6	4.0	
2730-M03a-16	9	1584	19	0.23405	28.39	0.03195	1.89	0.07	202.8	3.9	214	65		202.8	3.9	
2730-M03a-17	12	1546	14	0.18115	51.05	0.03196	1.94	0.04	202.8	4.0	169	90		202.8	4.0	
2730-M03a-18	12	1651	12	0.23281	38.08	0.03211	1.62	0.04	203.7	3.3	213	86		203.7	3.3	
2730-M03a-19	15	1852	9	0.19034	43.99	0.03223	2.54	0.06	204.5	5.3	177	82		204.5	5.3	
2730-M03a-20	24	1445	6	0.27331	49.68	0.03229	3.07	0.06	204.8	6.4	245	129		204.8	6.4	
2730-M03a-21	14	1773	8	0.19060	7.76	0.03249	2.40	0.31	206.1	5.0	177	15		206.1	5.0	
2730-M03a-22	12	1102	10	0.16871	39.70	0.03253	2.52	0.06	206.4	5.3	158	66		206.4	5.3	
2730-M03a-23	9	2081	11	0.21319	14.80	0.03256	1.92	0.13	206.5	4.0	196	32		206.5	4.0	
2730-M03a-24	9	1761	10	0.27132	35.72	0.03259	2.22	0.06	206.7	4.7	244	94		206.7	4.7	
2730-M03a-25	10	2678	16	0.17055	33.97	0.03263	2.39	0.07	207.0	5.0	160	57		207.0	5.0	
2730-M03a-26	8	1189	17	0.19358	15.03	0.03268	3.07	0.20	207.3	6.5	180	29		207.3	6.5	
2730-M03a-27	14	7502	12	0.28776	18.72	0.03270	1.46	0.08	207.4	3.1	257	53		207.4	3.1	
2730-M03a-28	10	4406	14	0.28972	29.08	0.03272	1.78	0.06	207.5	3.8	258	82		207.5	3.8	
2730-M03a-29	10	16642	10	0.23002	28.44	0.03290	1.85	0.07	208.6	3.9	210	64		208.6	3.9	
2730-M03a-30	12	1244	15	0.18617	41.88	0.03318	1.82	0.04	210.4	3.9	173	76		210.4	3.9	
2730-M03a-31	7	1786	14	0.21481	22.86	0.03322	3.48	0.15	210.7	7.4	198	49		210.7	7.4	
2730-M03a-32	13	2352	11	0.23386	21.57	0.03333	1.55	0.07	211.3	3.3	213	50		211.3	3.3	
2730-M03a-33	15	7789	9	0.25611	19.91	0.03341	2.62	0.13	211.8	5.6	232	51		211.8	5.6	
2730-M03a-34	11	2969	11	0.21279	19.60	0.03350	2.69	0.14	212.4	5.8	196	42		212.4	5.8	
2730-M03a-35	11	1446	21	0.19779	62.51	0.03351	1.71	0.03	212.5	3.7	183	118		212.5	3.7	
2730-M03a-36	9	1926	14	0.27263	9.00	0.03351	2.72	0.30	212.5	5.9	245	25		212.5	5.9	
2730-M03a-37	10	1779	16	0.30870	45.42	0.03361	1.86	0.04	213.1	4.0	273	133		213.1	4.0	
2730-M03a-38	62	3913	6	0.24121	7.09	0.03364	1.53	0.22	213.3	3.3	219	17		213.3	3.3	
2730-M03a-39	9	1703	9	0.26682	36.00	0.03366	2.84	0.08	213.4	6.2	240	93		213.4	6.2	
2730-M03a-40	18	2189	7	0.24025	19.80	0.03367	1.71	0.09	213.5	3.7	219	47		213.5	3.7	
2730-M03a-41	10	1879	12	0.21472	45.67	0.03374	2.47	0.05	213.9	5.4	198	95		213.9	5.4	
2730-M03a-42	8	1068	20	0.20596	28.05	0.03375	2.31	0.08	213.9	5.0	190	57		213.9	5.0	
2730-M03a-43	5	2203	-210	0.22893	15.60	0.03394	1.86	0.12	215.2	4.1	209	36		215.2	4.1	
2730-M03a-44	8	4059	19	0.29140	110.19	0.03442	2.40	0.02	218.1	5.3	260	283		218.1	5.3	
2730-M03a-45	6	2175	14	0.20763	61.81	0.03449	3.27	0.05	218.6	7.3	192	123		218.6	7.3	
2730-M03a-46	7	2491	17	0.24698	53.59	0.03477	3.84	0.07	220.4	8.6	224	126		220.4	8.6	
2730-M03a-47	26	9356	4	0.26281	16.95	0.03484	1.45	0.09	220.7	3.3	237	44		220.7	3.3	
2730-M03a-48	9	970	9	0.18189	45.49	0.03512	2.60	0.06	222.5	5.9	170	81		222.5	5.9	
2730-M03a-49	17	2707	8	0.20294	23.85	0.03516	2.12	0.09	222.7	4.8	188	48		222.7	4.8	
2730-M03a-50	9	2302	9	0.26166	73.57	0.03602	3.10	0.04	228.1	7.2	236	179		228.1	7.2	

(continued)

TABLE 1. U-Pb ZIRCON GEOCHRONOLOGIC ANALYSES BY LASER-ABLATION MULTICOLLECTOR ICP MASS SPECTROMETRY (continued)

	Isotopic ratios								Apparent ages (Ma)							
	U (ppm)	$\frac{^{206}\text{Pb}_m}{^{204}\text{Pb}}$	U/Th	$\frac{^{207}\text{Pb}^*}{^{235}\text{U}}$	± (%)	$\frac{^{206}\text{Pb}^*}{^{238}\text{U}}$	± (%)	error corr.	$\frac{^{206}\text{Pb}^*}{^{238}\text{U}}$	± (Ma)	$\frac{^{207}\text{Pb}^*}{^{235}\text{U}}$	± (Ma)	$\frac{^{206}\text{Pb}^*}{^{207}\text{Pb}^*}$	± (Ma)	Age	± (Ma) 1 σ
3626-C01-1c	85	828	1.7	0.19587	20.0	0.02673	1.9	0.10	170.0	3.3	181.6	39.0		170.0	3.3	
3626-C01-2c	37	208	2.0	0.22444	33.6	0.02829	2.4	0.07	179.8	4.4	205.6	73.9		179.8	4.4	
3626-C01-4c	39	408	1.9	0.86352	76.2	0.02811	3.8	0.05	178.7	6.9	632.0	513.4		178.7	6.9	
3626-C01-5c	96	924	1.6	0.12939	35.7	0.02778	1.7	0.05	176.6	3.0	123.6	45.8		176.6	3.0	
3626-C01-6c	44	364	2.4	0.11012	47.9	0.02766	3.0	0.06	175.9	5.3	106.1	52.2		175.9	5.3	
3626-C01-7c	33	332	2.2	0.13648	113.0	0.02610	2.8	0.02	166.1	4.7	129.9	145.7		166.1	4.7	
3626-C01-9c	79	884	2.4	0.15824	26.7	0.02724	2.6	0.10	173.2	4.6	149.2	42.0		173.2	4.6	
3626-C01-10c	78	876	2.2	0.11808	49.2	0.02776	1.4	0.03	176.5	2.6	113.3	57.4		176.5	2.6	
3626-C01-11c	25	512	2.4	0.24614	1000.2	0.02743	3.7	0.00	174.4	6.6	223.4	1260.9		174.4	6.6	
3626-C01-12c	48	600	1.7	0.21316	330.9	0.02545	3.1	0.01	162.0	5.1	196.2	541.9		162.0	5.1	
3626-C01-13c	30	500	2.2	5.36196	470.5	0.02489	5.4	0.01	158.5	8.7	1878.8	3317.0		158.5	8.7	
3626-C01-15c	70	2076	1.5	0.21518	428.1	0.02625	1.4	0.00	167.0	2.3	197.9	663.0		167.0	2.3	
3626-C01-16c	80	1976	2.2	0.51371	77.2	0.02857	2.3	0.03	181.6	4.1	420.9	339.3		181.6	4.1	
3626-C01-17c	84	2076	1.9	0.21500	39.6	0.02894	3.3	0.08	183.9	6.1	197.7	83.0		183.9	6.1	
3626-C01-18c	28	536	2.3	0.59538	69.7	0.02582	6.8	0.10	164.3	11.3	474.3	352.4		164.3	11.3	
3626-C01-19c	209	4020	1.0	0.17112	9.7	0.02582	1.5	0.16	164.3	2.6	160.4	16.8		164.3	2.6	
3626-C01-20c	42	1328	3.6	0.26032	70.9	0.02522	3.2	0.05	160.6	5.2	234.9	171.9		160.6	5.2	
3626-C01-21r	36	660	2.5	0.53107	52.2	0.02764	5.3	0.10	175.8	9.4	432.5	248.3		175.8	9.4	
3626-C01-22r	72	1284	2.3	0.11638	69.8	0.02655	1.4	0.02	168.9	2.3	111.8	79.3		168.9	2.3	
3626-C01-23r	51	760	1.7	0.59747	16.5	0.02849	2.4	0.15	181.1	4.4	475.6	95.7		181.1	4.4	
3626-C01-24r	51	1220	3.2	0.40554	36.0	0.02572	2.1	0.06	163.7	3.4	345.7	138.4		163.7	3.4	
3626-C01-25r	43	976	2.2	0.40783	43.1	0.02868	2.7	0.06	182.3	5.0	347.3	164.3		182.3	5.0	
3626-C01-26r	93	1788	2.4	0.22095	15.3	0.02706	2.0	0.13	172.1	3.5	202.7	33.7		172.1	3.5	
3626-C01-27r	55	1304	1.8	1.17253	163.1	0.02834	1.3	0.01	180.2	2.4	787.8	1085.3		180.2	2.4	
3626-C01-28r	79	1996	1.6	0.15466	16.1	0.02598	1.6	0.10	165.3	2.6	146.0	24.9		165.3	2.6	
3626-C01-29r	34	568	3.0	0.16675	125.0	0.02583	4.3	0.03	164.4	7.1	156.6	192.3		164.4	7.1	
3626-C01-30r	36	644	2.3	1.81769	491.6	0.02507	3.9	0.01	159.6	6.3	1051.9	2331.4		159.6	6.3	
3626-C01-31r	63	1148	2.6	0.21837	66.2	0.02642	1.8	0.03	168.1	3.1	200.6	137.2		168.1	3.1	
3626-C01-33r	62	1224	2.5	0.28318	21.7	0.02770	1.7	0.08	176.1	3.0	253.2	60.5		176.1	3.0	
3626-C01-35r	44	972	1.8	0.19991	92.0	0.02654	2.5	0.03	168.8	4.3	185.0	171.5		168.8	4.3	

Notes: r and c refer to rim and core analyses. Age column refers to interpreted age of grain, using $^{206}\text{Pb}/^{238}\text{U}$ age if the $^{206}\text{Pb}/^{238}\text{U}$ age is <800 Ma and the $^{207}\text{Pb}/^{206}\text{Pb}$ age for grains >800 Ma.

*indicates corrected ratio or age.

See Analytical Techniques section for more details.

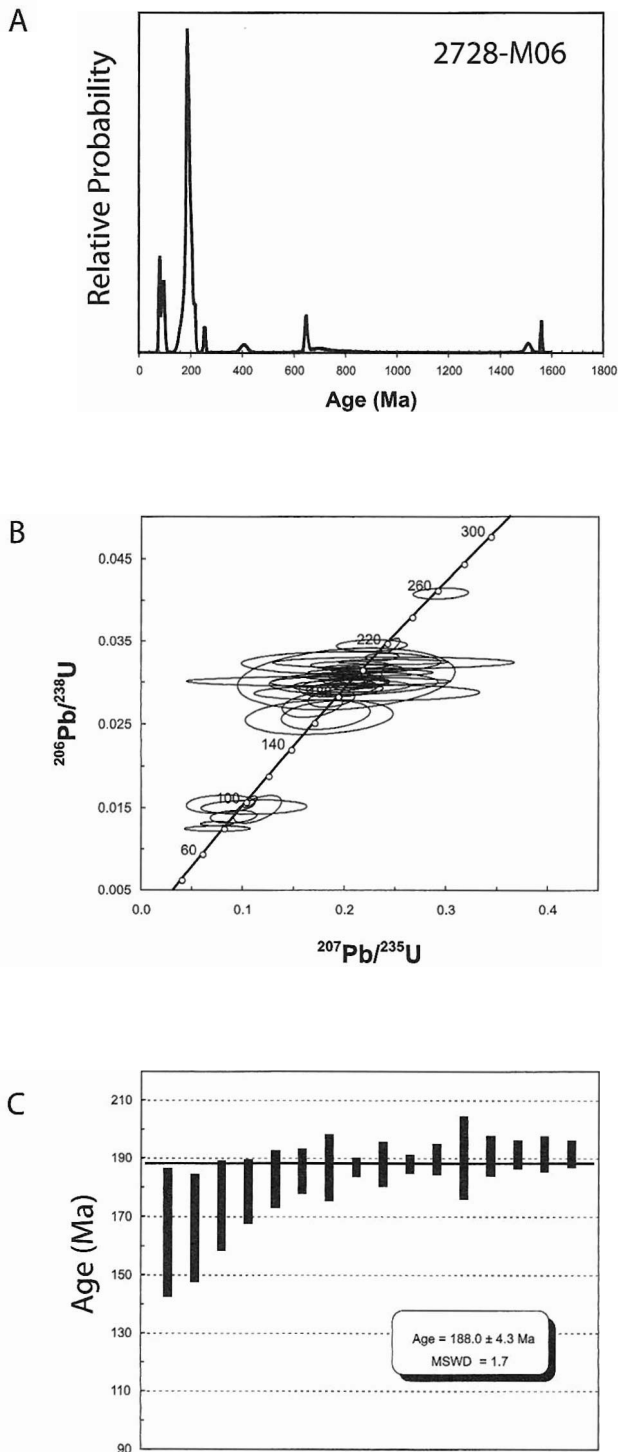


Figure 4. U-Pb data from sample 2728-M06 ($n = 46$). (A) Relative probability plot, (B) concordia diagram, (C) weighted mean age. Locality: UTM Zone 5, 6468850E, 337399N.

and rounded grains to larger angular fragments. The data include seven young zircon ages (100–80 Ma) that were from euhedral zircons. The most significant peak on a probability distribution diagram (Fig. 4) includes 16 grains and has a weighted mean $^{206}\text{Pb}/^{238}\text{U}$ age of 188 ± 4 Ma (MSWD = 1.7). There are 14 zircons with $^{206}\text{Pb}/^{238}\text{U}$ ages ranging from 193 to 218 Ma. All of the grains in this sample with ages <250 Ma are concordant. Eight grains have ages between 258 and 1563 Ma, and the four concordant zircons in this group have ages of 411 Ma, ca. 650 Ma, and 1512 Ma.

A total of 25 zircons were dated from sample 2728-M05 (Fig. 5). One zircon had a young $^{206}\text{Pb}/^{238}\text{U}$ age of 84 Ma. A weighted mean of the zircons comprising the most significant peak on the probability distribution plot (14 grains) is 181 ± 6 Ma (MSWD = 1.7). This is the same age within error of the youngest peak from sample 2728M-06. Ten older grains yielded concordant or near concordant ages between 215 Ma and 2637 Ma.

Twenty-nine zircons were analyzed from sample 2731-P02 (Fig. 6). The youngest grain has a $^{206}\text{Pb}/^{238}\text{U}$ age of 145 ± 12 Ma. The highest peak on the relative probability diagram is at ca. 169 Ma. Another prominent peak based on data from seven zircons is at 208 Ma. Ten older grains have concordant ages from 617 to 224 Ma.

Western Chugach Mountains/Knik Terrane

Thirty-seven zircons were analyzed from sample 2709-B08. Grains range in length from 100 to 250 μm and have aspect ratios of 3:2–2:1 and are generally euhedral or subhedral. Both cores and rims were analyzed; rim analyses were generally younger and high in U (10–20 \times the values for the cores). The analyses yield a range of $^{206}\text{Pb}/^{238}\text{U}$ ages from 214 to 185 Ma (Fig. 7). The three ages younger than 190 Ma all have high U concentrations (>1000 ppm), suggesting Pb loss may have occurred. The analyses are concordant within the uncertainties in the data.

Talkeetna Formation

We analyzed 50 zircons from sample 2730-M03a (Fig. 8). All of the zircons analyzed have low U concentrations. All analyses were concordant and represent a broad population with a weighted mean $^{206}\text{Pb}/^{238}\text{U}$ age of 207 ± 5 Ma (MSWD = 3.1).

Tuxedni Group/Chinitna Formation

A combination of cores and rims from 30 zircons in sample 3626-C01 were analyzed (Fig. 9). All zircons are euhedral and range in length from 200 to 300 μm with aspect ratios ranging from 2:1 to 5:1. There were four grains that yielded both core and rim ages. In each of these grains, the core and rim ages were indistinguishable within 2σ uncertainty. The weighted mean of all of the core ages is the same as the mean of the rim ages. The data have a weighted mean $^{206}\text{Pb}/^{238}\text{U}$ age of 171 ± 4 Ma (MSWD = 3.1), but the high MSWD suggests that there may be a combination of two or more zircon populations. The ages are not correlated to U concentrations. When the data were evaluated as two

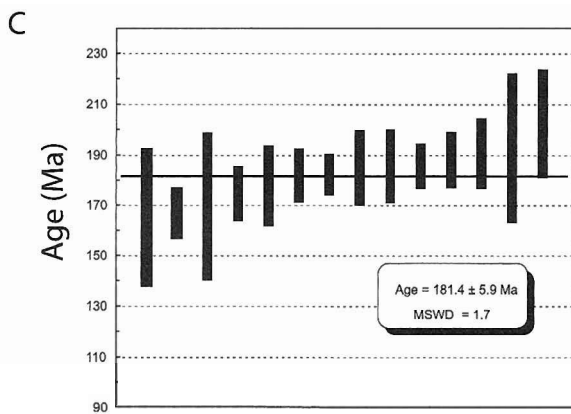
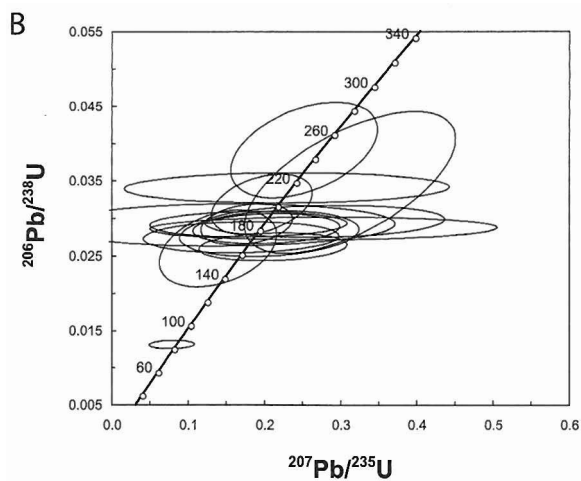
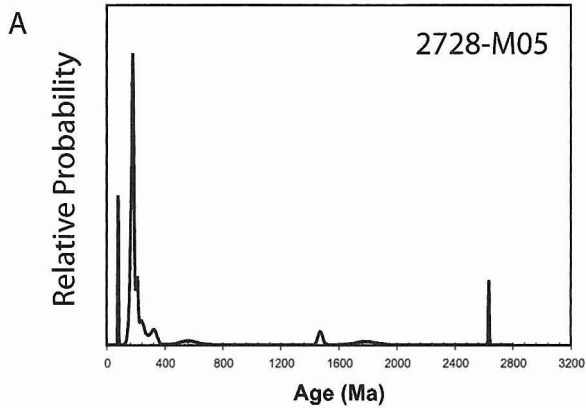


Figure 5. U-Pb data from sample 2728-M05 (n = 25). (A) Relative probability plot, (B) concordia diagram, (C) weighted mean age. Locality: UTM Zone 5, 6501019E, 349879N.

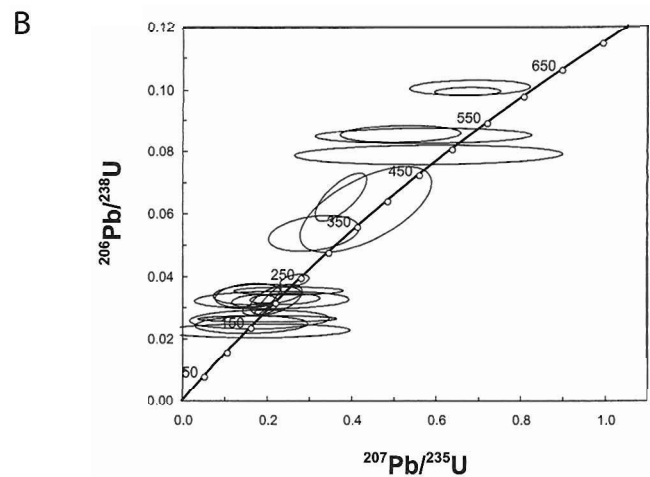
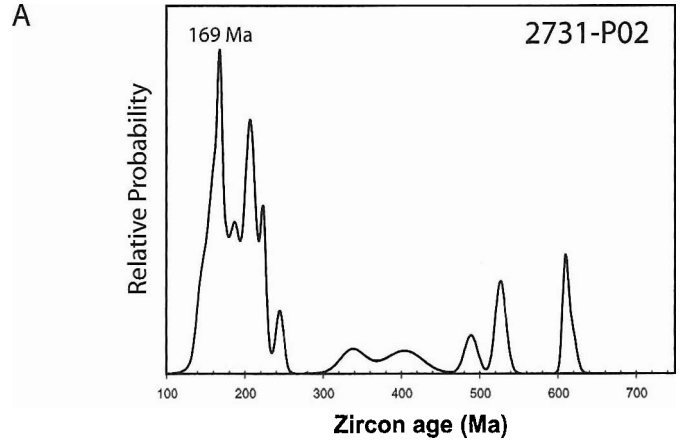


Figure 6. U-Pb data from sample 2731-P02 (n = 29). (A) Relative probability plot, (B) concordia diagram. Locality: UTM Zone 5, 6635343E, 479633N.

separate populations using the “unmix” routine of Isoplot (Ludwig, 2002), a younger population of 167 ± 4 Ma (MSWD = 0.75) and an older population of 178 ± 4 Ma (MSWD = 0.49) were discriminated.

DISCUSSION

The new U-Pb analyses provide important constraints on the timing of Talkeetna arc magmatism and the role of older (Archean–Triassic) material in the development of the Jurassic Talkeetna arc. In the following section we discuss the interpretation of the U-Pb data and its implications. All of the samples in this study except the volcanic rock from the base of the Talkeetna Formation (sample 2730-M03a) have multiple statistically significant zircon U-Pb age populations. In interpreting these age spectra we note that (1) insufficient zircons were analyzed to fully characterize the entire zircon population, and (2) Archean to Triassic

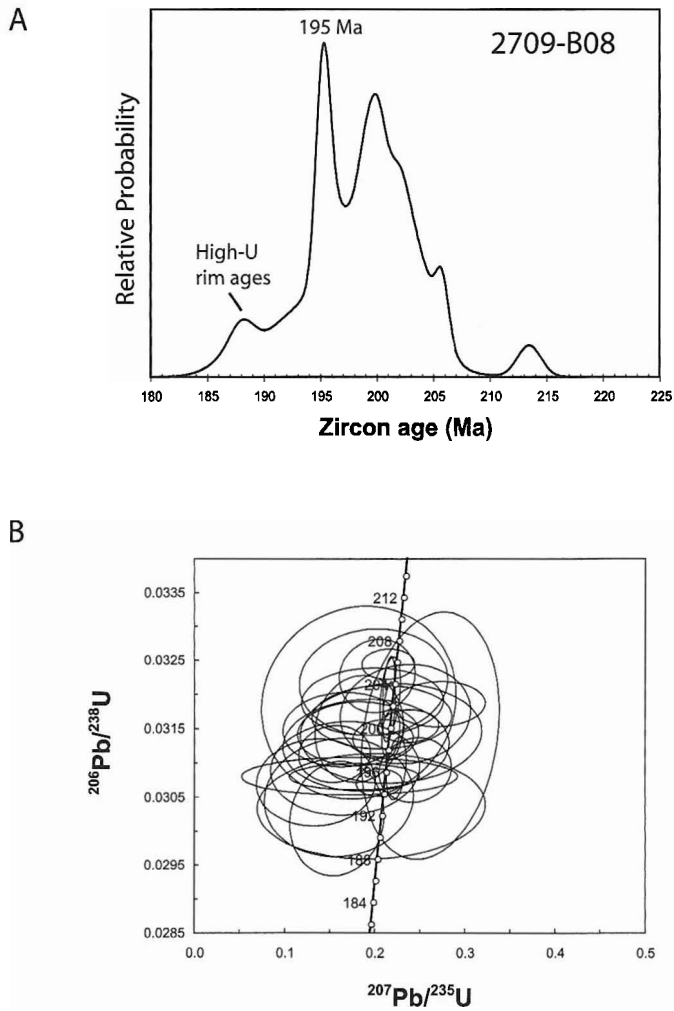


Figure 7. U-Pb data from sample 2709-B08 (n = 37). (A) Relative probability plot, (B) concordia diagram. Locality: UTM Zone 6, 6833731E, 411147N.

components are generally too poorly represented to identify the source area.

U-Pb Age Determinations

Prearc Samples

The Kakhonak Complex of Detterman and Reed (1980) consists of metamorphosed equivalents of other mapped units in the Iliamna quadrangle. Because of metamorphism and deformation, the original nature of the protoliths is obscured. Despite being originally interpreted as mainly consisting of prearc rocks, Detterman and Reed (1980) recognized that the Kakhonak Complex probably contained rocks of diverse ages and tectonic significance, including prearc successions such as Triassic (Norian?) greenstone, synarc rocks such as the Early Jurassic Talkeetna Formation, and possibly some metamorphosed postarc sequences.

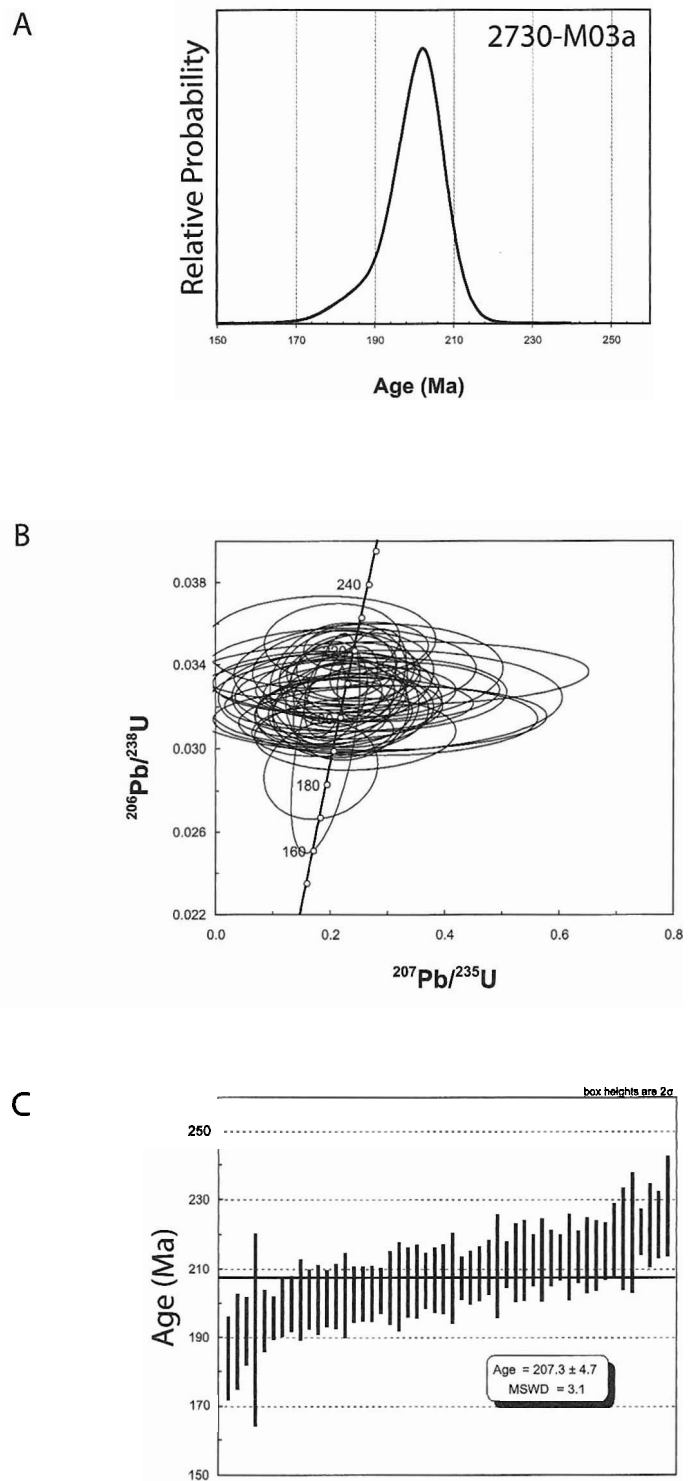


Figure 8. U-Pb data from sample 2730-M03a (n = 50). (A) Relative probability plot, (B) concordia diagram, (C) weighted mean age. Locality: UTM Zone 5, 6667712E, 503136N.

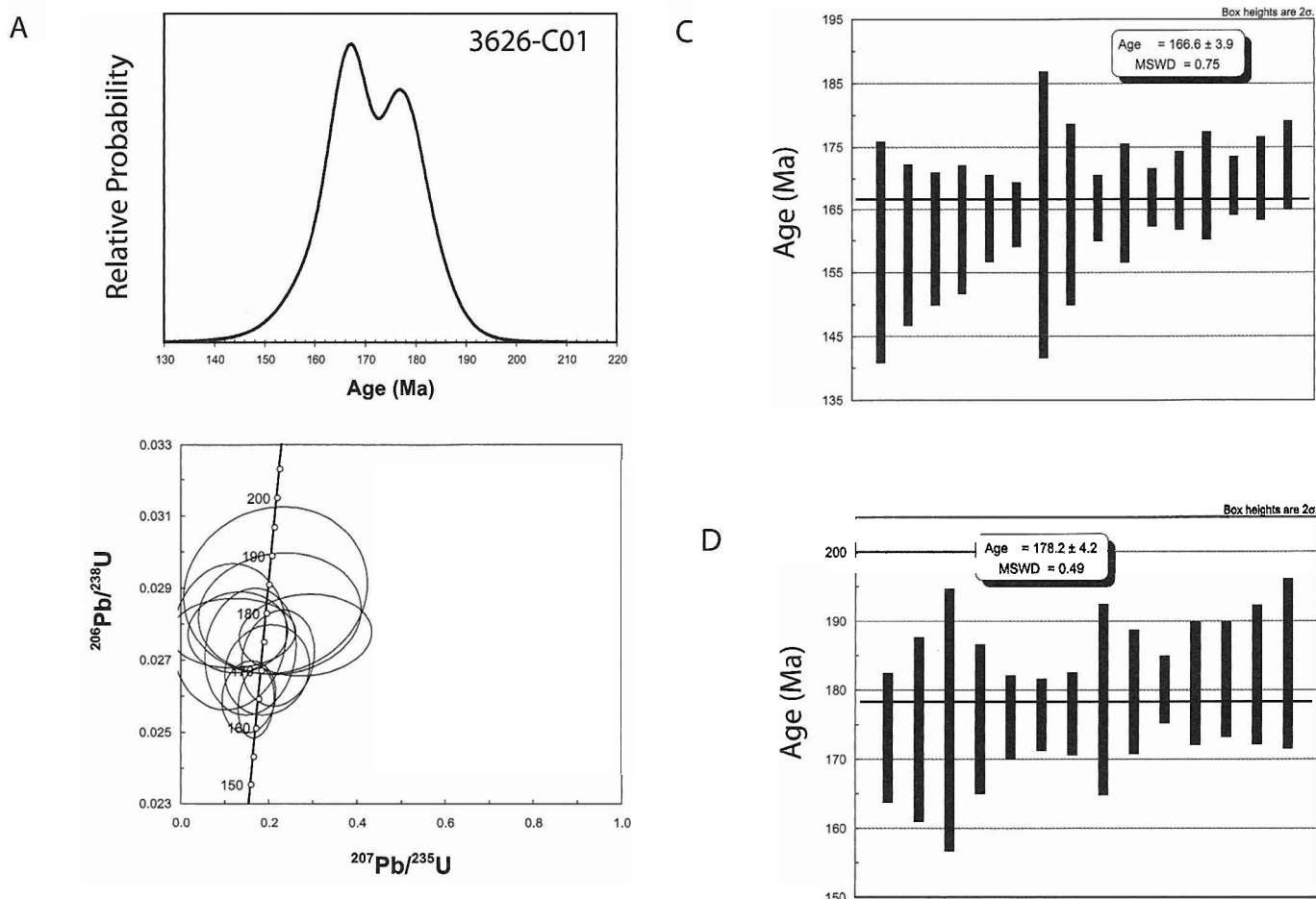


Figure 9. U-Pb data from sample 3626-C01 ($n = 30$). (A) Relative probability plot; (B) concordia diagram; analyses with $^{207}\text{Pb}/^{235}\text{U}$ ratio uncertainties of $>40\%$ were not plotted; (C) weighted mean age of young population; (D) weighted mean age of older population. Locality: UTM Zone 6, 6894311E, 465049N.

Our new U-Pb zircon ages provide constraints on the true affinity of different parts of the Kakhonak Complex. The detrital zircon signatures of Kakhonak Complex samples are particularly interesting because the dated samples come from mapped plutonic screens and roof pendants from the Jurassic batholith and therefore can provide information of the tectonic setting of the Talkeetna arc during active magmatism

The three samples from the Kakhonak Complex have zircons ranging from Archean and Proterozoic to Cretaceous ages. The youngest zircons from sample 2728-M06 range from 100 to 80 Ma. These were likely derived from small Cretaceous dikes, similar to the dike seen in sample 2728-M05, although these features were not observed in the hand samples prior to sample processing. The largest population in sample 2728-M06 has an age of 188 ± 4 Ma, and older components record Proterozoic to Paleozoic ages. The distribution of ages within the sample is consistent with a volcaniclastic or sedimentary origin with a maximum

depositional age of 188 Ma. The oldest dated Jurassic pluton in this part of the Alaska Peninsula has an age of 183.3 ± 0.1 Ma (Rioux et al., 2005) and U-Pb analyses from the base of the Talkeetna Formation indicate that active arc volcanism started between 207 Ma (this study) and 198 Ma (Pálffy et al., 1999). Sedimentary units are common in the Talkeetna Formation (Clift et al., 2005a), and this sample may represent either a sedimentary or volcaniclastic layer within the arc volcanic sequence, which was metamorphosed during Mid-Jurassic plutonism. The oldest grains in sample 2728-M06 are Proterozoic to Paleozoic and the range of ages suggests that the protolith is likely a volcaniclastic or sedimentary rock with a maximum depositional age of 188 Ma.

The youngest Jurassic zircon population in sample 2728-M05 is 181 ± 6 Ma, again suggesting a maximum depositional age that is synchronous with Talkeetna arc volcanism. The texture and mineralogy (quartz + plagioclase) suggests that this rock

may be a metamorphosed and deformed intermediate to felsic volcanic rock and is consistent with it being part of the upper Talkeetna Formation. It is located near a pluton dated at 178.7 ± 0.3 Ma (M. Rioux, 2006, personal commun.), and thus it is clear that magmatism was active at this time. The ten grains with Archean-Triassic ages require the assimilation of inherited older components. The single 84 Ma age is attributed to the cross-cutting dike in this sample.

Sample 2731-P02 contained a range of zircons with Jurassic to Proterozoic ages. The youngest population in the sample suggests a maximum depositional age of ca. 169 Ma. Fossil successions bracket the top of the Talkeetna Formation between the late Toarcian and middle Bajocian (180.1 ± 4.0 to 169.2 ± 4.0 Ma; Grantz et al., 1963; Imlay, 1984; Gradstein et al., 1995). This sample therefore represents a sedimentary layer from either the top of the Talkeetna Formation or the overlying Tuxedni Group. The range of Early Jurassic to Late Triassic (ca. 208 Ma) ages in the sample may reflect incorporation of detritus from the oldest Talkeetna Formation rocks during deposition, including a young population at ca. 169 Ma that is younger than most of the Triassic protoliths of the Kakhonak Complex and is near the age of the youngest Talkeetna Formation rocks (typically Toarcian or younger).

Synarc Samples

Sample 2730-M03a was collected from a unit at the base of the Talkeetna Formation and yielded a single population of 50 zircons with a weighted mean age of 207 ± 5 Ma. The high MSWD (3.1) for the analyses and asymmetric shape of the distribution are consistent with Pb loss in some grains. The data suggest a Late Triassic initiation of Talkeetna arc volcanism in this area compared to the Early Jurassic age determined by Pálffy et al. (1999) at Puale Bay. The abundance of zircons within a single age population argues against the rock's being a younger volcanic rock with Triassic inheritance but does not rule out this possibility.

The greenschist-facies metabasalt from the western Chugach Mountains (2709-B08) yielded zircons with a range of ages from 214 to 185 Ma. The complex age systematics in a metabasaltic composition may reflect Pb loss from some grains, inheritance of xenocrystic older zircon, or both. The data are consistent with the zircons' being derived from the Talkeetna Formation or Jurassic plutons. These results constrain the age of the protolith to <185 Ma and are consistent with the sample's representing a metamorphosed Talkeetna Formation mafic volcanic rock.

Postarc Sample

Sample 3626-C01, the volcanoclastic sandstone from the Middle Jurassic sedimentary rocks overlying the Talkeetna Formation recorded ages from 183.9 to 158.5 Ma. As discussed above, the data appear to reflect mixing of two populations with ages of 178 ± 4 Ma and 167 ± 4 Ma. These data constrain the depositional age of the sedimentary rocks to <167 Ma and reflect the local cessation of Talkeetna arc volcanism. The age is consis-

tent with the faunal evidence that brackets the termination of arc volcanism between the late Toarcian and middle Bajocian (as previously discussed).

The Duration of Talkeetna Arc Volcanism

The samples analyzed in this study bracket the full extent of the Talkeetna Formation and constrain the timing of Talkeetna arc volcanism. Sample 2730-M03a was collected from the base of the volcanic section of the Alaska Peninsula and suggests that initial arc volcanism began by 207 ± 5 Ma in this area. In a separate section in the Talkeetna Mountains, a volcanoclastic sandstone (sample 3626-C01) overlying the Talkeetna Formation volcanic rocks records a depositional age of <167 Ma. This age does not directly constrain the termination of arc volcanism but is consistent with existing faunal evidence that indicate that the Talkeetna Formation is overlain by middle Bajocian sediments. Taken together, the data suggest that the arc was active for ca. 40 m.y. Uranium-Pb ages from arc plutonic rocks range from 217 ± 10 Ma on Kodiak Island (Roeske et al., 1989) to 153 Ma in the Talkeetna Mountains (Rioux et al., 2007) in agreement with the timespan of arc volcanism.

Inheritance in Talkeetna Arc Magmatism

A significant finding of this study is the identification of Paleozoic to Proterozoic zircons in metavolcanic and metasedimentary plutonic screens or roof pendants along the Alaska Peninsula. Pálffy et al. (1999) also noted the presence of Proterozoic inherited zircons in their U-Pb dating of Talkeetna Formation tuffs in the Puale Bay area. The presence of older material suggests that the volcanic and plutonic section on the Alaska Peninsula formed in close proximity to older continental material.

In contrast, data from the eastern exposures of the arc in the Chugach and Talkeetna Mountains record little evidence for pre-existing continental detritus. Existing U-Pb data from arc plutons in the Chugach and eastern Talkeetna Mountain record concordant or near concordant ages between 201–169 Ma. Only a single sample from the western Chugach Mountains, within the Knik River terrane, generated discordant data that indicate inheritance of Precambrian xenocrysts. Discordant analyses in the western Talkeetna Mountains are consistent with assimilation of Paleozoic Wrangellian crust into Jurassic arc magmas. Existing isotopic data from the Talkeetna arc further constrain the role of crustal assimilation in arc magmatism (Rioux et al., 2007; Greene et al., 2006; Clift et al., 2005a). Data from the Chugach and Talkeetna Mountains follow the trends of the U-Pb zircon analyses. In the Chugach Mountains and eastern Talkeetna Mountains, initial Nd and Sr ratios are similar to those from typical juvenile intraoceanic arc crust. In contrast, data from plutons in the central and western Talkeetna Mountains, closer to the Wrangellia Terrane margin (Fig. 1), record Nd and Sr isotopic values indicating assimilation of older Wrangellian crust

(Rioux et al., 2007). Isotopic ratios from the Alaska Peninsula overlap but extend to slightly lower ϵ_{Nd} than the arc-like ratios in the Chugach and eastern Talkeetna Mountains (Rioux et al., 2005).

The combination of the detrital zircon data with existing geochemical and geochronological data on igneous rocks from the arc suggests that there were along-strike variations in the tectonic setting of the Talkeetna arc. Data from the Chugach Mountains are consistent with formation in a typical intraoceanic setting, whereas the data from the Alaska Peninsula suggest that the arc in this region incorporated sediment that had a continentally derived clastic component. There is no Precambrian crust in the Peninsular terrane, requiring that any Precambrian zircons found as detrital grains in prearc sequences must be derived from a continent or continental fragment. These older detrital grains were mixed into the oceanic sedimentary rocks that predate the arc in the Alaska Peninsula area, but this continental-derived detritus did not constitute a sufficiently large source to significantly influence the isotope geochemistry of the Talkeetna arc magmas that passed through this clastic apron as the arc was built.

CONCLUSIONS

Detrital zircons from six metamorphic, volcanic, and sedimentary samples collected from pre-, syn-, and post-Talkeetna arc rocks in southwest Alaska were dated using LA-MC-ICP-MS geochronology. Three samples from the Kakhonak Complex in the Katmai, Iliamna, and Kenai quadrangles were dated. A metamorphosed intermediate to felsic volcanic rock yields a peak at 188 ± 4 Ma. A low-grade metamorphosed lithic quartz sandstone has a population of zircon ages at 181 ± 6 Ma. Based on their age and lithology, these two samples are interpreted as variably metamorphosed Talkeetna Formation rocks. A siliceous metasedimentary rock has a range of ages from 617 to 145 Ma suggesting it may have been deposited after arc volcanism ceased.

A sample from a Talkeetna Formation volcanic breccia yielded a zircon population dated at 207 ± 5 Ma. This age is older than ages reported from the top of the Kamishak Formation immediately underlying the Talkeetna Formation in Puale Bay (Pálffy et al., 1999). A greenschist-facies metabasalt yielded zircon ages ranging from 214 to 185 Ma. A volcanoclastic sandstone overlying the Talkeetna Formation in the Talkeetna Mountains yielded a population at 167 ± 4 Ma. The duration of Talkeetna arc magmatism in this area was at least 40 m.y.

Three of the four samples from the Alaska Peninsula contained older detrital zircons with ages ranging from Archean to Triassic, but too few pre-Jurassic ages were determined to be able to identify potential source areas.

ACKNOWLEDGMENTS

This project was funded from National Science Foundation Earth Sciences (Continental Dynamics) program grant EAR-9910899. Kelemen was also partially supported by NSF grants EAR-0087706, EAR-0409092, OCE-0426160, and OCE-0242233.

This paper was improved by reviews by Jeff Trop, John Aleinikoff, John Barbeau, and Colin Shaw.

REFERENCES CITED

- Amato, J.M., Bogar, M.J., Gehrels, G.E., Farmer, G.L., and McIntosh, W.C., 2007, this volume, The Tlikakila Complex in southern Alaska: A suprasubduction-zone ophiolite between the Wrangellia Composite terrane and North America, in Ridgway, K.D., Trop, J.M., Glen, J.M.G., and O'Neill, J.M., eds., Tectonic Growth of a Collisional Continental Margin: Crustal Evolution of Southern Alaska: Geological Society of America Special Paper 431, doi: 10.1130/2007.2431(10).
- Barbeau, D.L., Jr., Ducea, M.N., Gehrels, G.E., Kidder, S., Wetmore, P.H., and Saleeby, J.B., 2005, U-Pb detrital-zircon geochronology of northern Salinian basement and cover rocks: Geological Society of America Bulletin, v. 117, p. 466–481, doi: 10.1130/B25496.1.
- Bradley, D.C., Kusky, T.M., Haeussler, P.J., Karl, S.M., and Donley, D.T., 1999, Geologic map of the Seldovia quadrangle, south-central Alaska: U.S. Geological Survey Open-File Report 99-18.
- Burns, L.E., 1985, The Border Ranges ultramafic and mafic complex, south-central Alaska: Cumulate fractionates of island arc volcanics: Canadian Journal of Earth Sciences, v. 22, no. 1020–1038.
- Clift, P.D., Draut, A.E., Kelemen, P.B., Blusztajn, J., and Greene, A., 2005a, Stratigraphic and geochemical evolution of an oceanic arc upper crustal section: The Jurassic Talkeetna Volcanic Formation, south-central Alaska: Geological Society of America Bulletin, v. 117, p. 902–925, doi: 10.1130/B25638.1.
- Clift, P.D., Pavlis, T., DeBari, S.M., Draut, A.E., Rioux, M., and Kelemen, P.K., 2005b, Subduction erosion of the Jurassic Talkeetna-Bonanza arc and the Mesozoic accretionary tectonics of western North America: Geology, v. 33, p. 881–884, doi: 10.1130/G21822.1.
- Connelly, W., and Moore, J., 1979, Geologic map of the northwest side of Kodiak and adjacent islands, Alaska: U.S. Geological Survey Miscellaneous Field Studies Map, v. MF-1057.
- Csejtey, B., Jr., Nelson, W.H., Jones, D.L., Silberling, N.J., Dean, R.M., Morris, M.S., Lanphere, M.A., Smith, J.G., and Silberling, M.L., 1978, Reconnaissance geologic map and geochronology, Talkeetna Mountains quadrangle, northern part of Anchorage quadrangle, and southwest corner of Healy quadrangle, Alaska: U.S. Geological Survey Open-File Report 78-558A.
- DeBari, S.M., and Coleman, R.G., 1989, Examination of the deep levels of an island arc: Evidence from the Tonsina ultramafic-mafic assemblage, Tonsina, Alaska: Journal of Geophysical Research, v. 94, p. 4373–4391.
- Detterman, R.L., and Hartsock, J.K., 1966, Geology of the Iniskin-Tuxedni region, Alaska, U.S. Geological Survey Professional Paper 512, 78 p.
- Detterman, R.L., and Reed, B.L., 1980, Stratigraphy, structure, and economic geology of the Iliamna Quadrangle, Alaska: U.S. Geological Survey Bulletin 1368-B, p. B1–B86.
- Detterman, R.L., Hudson, T., Plafker, G., Tysdal, R.G., and Hoare, J.M., 1976, Reconnaissance geologic map along the Bruin Bay and Lake Clark faults in the Kenai and Tyonek quadrangles, Alaska: U.S. Geological Survey Open-File Report 76-477.
- Gradstein, F.M., and Ogg, J.A., 1996, A Phanerozoic time scale: Episodes, v. 19, p. 3–5.
- Gradstein, F.M., Agterberg, F.P., Ogg, J.G., Hardenbol, J., van Veen, P., Thierry, J., and Huang, Z., 1995, A Triassic, Jurassic and Cretaceous time scale, in Berggren, W.A., Kent, D.V., Aubry, M.-P., and Hardenbol, J., eds., Geochronology, time scales, and global stratigraphic correlation, Society for Sedimentary Geology Special Publication 54, p. 95–126.
- Grantz, A., Thomas, H., Stern, T.W., and Sheffey, N.B., 1963, Potassium-argon and lead-alpha ages for stratigraphically bracketed plutonic rocks in the Talkeetna Mountains, Alaska: U.S. Geological Survey Professional Paper 475-B, p. 56–59.
- Greene, A.R., DeBari, S.M., Kelemen, P.B., Blusztajn, J., and Clift, P.D., 2006, A detailed geochemical study of island arc crust: The Talkeetna arc section,

- south-central Alaska: *Journal of Petrology*, v. 47, p. 1051–1093, doi: 10.1093/petrology/eg1002.
- Hillhouse, J., 1977, Paleomagnetism of the Triassic Nikolai Greenstone, McCarthy Quadrangle, Alaska: *Canadian Journal of Earth Sciences*, v. 14, p. 2578–2592.
- Imlay, R.W., 1984, Early and middle Bajocian (Middle Jurassic) ammonites from southern Alaska, U.S. Geological Survey Professional Paper 1322, 38 p.
- Jones, D.L., Silberling, N.J., Coney, P.J., and Plafker, G., 1987, Lithotectonic terrane map of Alaska (west of the 41st meridian): U.S. Geological Survey Miscellaneous Field Studies Map MF-874, scale 1:2,500,000.
- Little, T.A., and Naeser, C.W., 1989, Tertiary tectonics of the Border Ranges fault system, Chugach Mountains, Alaska: Deformation and uplift in a forearc setting: *Journal of Geophysical Research*, v. 94, p. 4333–4359.
- Ludwig, K.R., 2002, Isoplot/Ex, a geochronology toolkit for Microsoft Excel: Berkeley Geochronology Center Special Publication 1.
- Nelson, W.H., Carlson, C., and Case, J.E., 1983, Geologic map of the Lake Clark quadrangle, Alaska: U.S. Geological Survey Map MF-1114-A, scale 1:250,000.
- Newberry, R., Burns, L., and Pessel, P., 1986, Volcanogenic massive sulfide deposits and the “missing complement” to the calc-alkaline trend: Evidence from the Jurassic Talkeetna island arc of southern Alaska: *Economic Geology and the Bulletin of the Society of Economic Geologists*, v. 81, p. 951–960.
- Nokleberg, W.J., Plafker, G., and Wilson, F.H., 1994, Geology of south-central Alaska, in Plafker, G., and Berg, H.C., eds., *The Geology of Alaska: Boulder, Colorado*, Geological Society of America, *Geology of North America*, v. G-1, p. 311–366.
- Pálffy, J., Smith, P.L., Mortensen, J.K., and Friedman, R.M., 1999, Integrated ammonite biochronology and U-Pb geochronometry from a basal Jurassic section in Alaska: *Geological Society of America Bulletin*, v. 111, p. 1537–1549, doi: 10.1130/0016-7606(1999)111<1537:IABAUP>2.3.CO;2.
- Pavlis, T., 1982, Origin and age of the Border Ranges fault of southern Alaska and its bearing on the late Mesozoic tectonic evolution of Alaska: *Tectonics*, v. 1, p. 343–368.
- Pavlis, T., 1983, Pre-Cretaceous crystalline rocks of the western Chugach Mountains, Alaska: Nature of the basement of the Jurassic Peninsular Terrane: *Geological Society of America Bulletin*, v. 94, p. 1329–1344, doi: 10.1130/0016-7606(1983)94<1329:PCROTW>2.0.CO;2.
- Pavlis, T., Monteverde, D.H., Bowman, J.R., Rubenstone, J.L., and Reason, M.D., 1988, Early Cretaceous near-trench plutonism in southern Alaska: A tonalite-trondhjemite intrusive complex injected during ductile thrusting along the Border Ranges Fault system: *Tectonics*, v. 7, p. 1179–1199.
- Plafker, G., Nokleberg, W.J., and Lull, J.S., 1989, Bedrock geology and tectonic evolution of the Wrangellia, Peninsular, and Chugach terranes along the Trans-Alaska Crustal Transect in the northern Chugach Mountains and southern Copper River basin, Alaska: *Journal of Geophysical Research*, v. 94, p. 4255–4295.
- Reed, B.L., and Lanphere, M.A., 1973, Alaska-Aleutian Range batholith: Geochronology, chemistry, and relation to circum-Pacific plutonism: *Geological Society of America Bulletin*, v. 84, p. 2583–2610, doi: 10.1130/0016-7606(1973)84<2583:ARBGCA>2.0.CO;2.
- Riehle, J.R., Dettnerman, R.L., Yount, M.E., and Miller, J.W., 1993, Geologic map of the Mount Katmai quadrangle and adjacent parts of the Naknek and Afognak quadrangles, Alaska: U.S. Geological Survey Miscellaneous Investigations Series Map, v. I-2204.
- Rioux, M., Hacker, B., Mattinson, J., Kelemen, P., Blusztajn, J., Hanghoj, K., and Amato, J., 2005, Tectonic and geochemical evolution of the accreted Talkeetna Arc, south-central Alaska: Implications for a type section of intra-oceanic arc crust: *Eos (Transactions, American Geophysical Union)*, v. 86, p. Abstract V44C-07.
- Rioux, M., Hacker, B., Mattinson, J., Kelemen, P., Blusztajn, J., and Gehrels, G., 2007, The magmatic development of an intra-oceanic arc: High-precision U-Pb zircon and whole-rock isotopic analyses from the accreted Talkeetna arc, south-central Alaska: *Geological Society of America Bulletin*, v. 119 (in press).
- Roeske, S.M., Mattinson, J., and Armstrong, R.L., 1989, Isotopic ages of glaucophane schists on the Kodiak Islands, southern Alaska, and their implications for the Mesozoic tectonic history of the Border Ranges fault system: *Geological Society of America Bulletin*, v. 101, p. 1021–1037, doi: 10.1130/0016-7606(1989)101<1021:IAOGSO>2.3.CO;2.
- Silberling, N.L., Jones, D.L., Monger, J.W.H., Coney, P.J., Berg, H.C., and Plafker, G., 1994, Lithotectonic terrane map of Alaska and adjacent parts of Canada, in Plafker, G., and Berg, H.C., eds., *The Geology of Alaska: Boulder, Colorado*, Geological Society of America, *Geology of North America*, v. G-1, pl. 3, scale 1:2,500,000.
- Sisson, V.B., and Onstott, T.C., 1986, Dating blueschist metamorphism: A combined $^{40}\text{Ar}/^{39}\text{Ar}$ and electron microprobe approach: *Geochimica et Cosmochimica Acta*, v. 50, p. 2111–2117, doi: 10.1016/0016-7037(86)90264-4.
- Stacey, J.S., and Kramers, J.D., 1975, Approximation of terrestrial lead isotope evolution by a two-stage model: *Earth and Planetary Science Letters*, v. 26, p. 207–221, doi: 10.1016/0012-821X(75)90088-6.
- Trop, J.M., Ridgway, K.D., Manuszak, J.D., and Layer, P., 2002, Mesozoic sedimentary-basin development on the allochthonous Wrangellia composite terrane, Wrangell Mountains basin, Alaska: A long-term record of terrane migration and arc construction: *Geological Society of America Bulletin*, v. 114, p. 693–717, doi: 10.1130/0016-7606(2002)114<0693:MSBDOT>2.0.CO;2.
- Trop, J.M., Szuch, D.A., Rioux, M., and Blodgett, R.B., 2005, Sedimentology and provenance of the Upper Jurassic Naknek Formation, Talkeetna Mountains, Alaska: Bearings on the accretionary tectonic history of the Wrangellia composite terrane: *Geological Society of America Bulletin*, v. 117, p. 570–588, doi: 10.1130/B25575.1.
- Wallace, W.K., Hanks, C.L., and Rogers, J.F., 1989, The southern Kahiltina terrane: Implications for the tectonic evolution of southwestern Alaska: *Geological Society of America Bulletin*, v. 101, p. 1389–1407, doi: 10.1130/0016-7606(1989)101<1389:TSKTIF>2.3.CO;2.
- Wang, J., Newton, C.R., and Dunne, L., 1988, Late Triassic transition from biogenic to arc sedimentation on the Peninsular terrane: Puale Bay, Alaska Peninsula: *Geological Society of America Bulletin*, v. 100, p. 1466–1478, doi: 10.1130/0016-7606(1988)100<1466:LTTFTB>2.3.CO;2.
- Wilson, F.H., Dover, J.H., Bradley, D.C., Weber, F.R., Bundtzen, T.K., and Haeussler, P.J., 1998, Geologic map of central (interior) Alaska: U.S. Geological Survey Open-File Report 98-133.
- Winkler, G.R., 1992, Geologic map and summary geochronology of the Anchorage $1^\circ \times 3^\circ$ quadrangle, southern Alaska: U.S. Geological Survey, Miscellaneous Investigation Series Map, v. I-2283.
- Winkler, G.R., Silberman, M.L., Grantz, A., Miller, R.J., and MacKevett, E.M., 1981, Geologic map and summary geochronology of the Valdez quadrangle, southern Alaska: U.S. Geological Survey Open-File Report 80-892-A.
- Zhang, N., and Blodgett, R., 2006, Alaska Paleontological Database: <http://www.alaskafossil.org/>.